Functionally dissecting the spermatogonial subpopulations in mouse postnatal development

Youngmin Song

Department of Medicine

Division of Experimental Medicine

McGill University, Montréal

July 2023

A thesis submitted to McGill University in partial fulfillment of the requirements of the degree of Master of Science (M.Sc.)

Abstract

Spermatogonial stem cells (SSCs) are the foundation of spermatogenesis and drive sperm production throughout adult life. They are a crucial resource for fertility preservation, particularly for prepubertal boys who undergo gonadotoxic treatment. While these patients do not produce sperm to cryopreserve, in theory, SSCs can be isolated from their testes before treatment and transplanted later to restore fertility. Using the mouse model, I determined the cell-surface immunophenotypes of SSCs during postnatal development, as a step towards purifying prepubertal SSCs. I prospectively isolated SSC-enriched germ cells at three stages of development (postnatal day 0-2, 8-9, and 16-18) using Fluorescent-Activated Cell Sorting (FACS). I identified various cell fractions at each stage by the expression of four surface markers: THY1, ITGA6, GFRA1, and KIT. Cells in each fraction were assayed for their regenerative activity in vivo, self-renewal activity in vitro, and the expression of genes important in SSC fate control. I discovered that prepubertal germ cells exhibited unique immunophenotypic profiles that are specific to each stage of development, allowing us to identify the cell fractions with different levels of SSC activity. Here, I found the highest level of SSC enrichment reported so far in pups from a cell fraction that I named “Fraction A”, with approximately one SSC in 18 cells from P8-9 Fraction A. By further fractionating with GFRA1 and KIT, I found that almost all subfractions retain SSC activity in vivo and in vitro, indicating that neither GFRA1 loss nor KIT gain is indicative of stem cell depletion, although GFRA1 is a widely accepted SSC marker while KIT a differentiation marker. However, THY1 loss did correspond to SSC depletion. Future studies could explore THY1 as a fate marker, considering that loss of THY1 expression most accurately reflects the exit of stem cell state, more so than GFRA1 loss or KIT gain. Furthermore, the GFRA1/KIT subfractions can be scrutinized in more detail with transcriptional profiling, particularly to discern the identity of GFRA1+ KIT+ cells. My study will serve as a useful resource for future SSC isolation studies such that pure or near-pure SSCs can be obtained.

Résumé

Les cellules souches spermatogoniales (SSC) sont à la base de la spermatogenèse et assurent la production de spermatozoïdes tout au long de la vie adulte. Elles constituent une ressource cruciale pour la préservation de la fertilité, en particulier pour les garçons prépubères qui subissent un traitement gonadotoxique. Bien que ces patients ne produisent pas de sperme à cryoconserver, il est théoriquement possible d'isoler les SSC de leurs testicules avant le traitement et de les transplanter ultérieurement pour restaurer la fertilité. Dans le but de purifier les SSC prépubères, j'ai utilisé un modèle murin pour déterminer les immunophénotypes de surface cellulaire des SSC pendant le développement postnatal. J'ai prospectivement isolé les cellules germinales enrichies en SSC, à trois stades de développement (0-2, 8-9, et 16-18 jours post-partum) en utilisant le tri cellulaire activé par fluorescence (FACS). J'ai identifié différentes fractions cellulaires à chaque stade en fonction de l'expression de quatre marqueurs de surface: THY1, ITGA6, GFRA1 et KIT. Les cellules de chaque fraction ont été testées pour leur activité régénératrice in vivo, leur activité d'auto-renouvellement in vitro et l'expression de gènes importants dans le contrôle de la différentiation des SSC. J'ai découvert que les cellules germinales prépubères présentaient des profils immunophénotypiques uniques, spécifiques à chaque stade de développement, ce qui nous a permis d'identifier les fractions cellulaires présentant différents niveaux d'activité des SSC. J'ai trouvé le plus haut niveau d'enrichissement en SSC rapporté jusqu'à présent chez les souriceaux à partir d'une fraction cellulaire que j'ai nommée "Fraction A"; plus de 250 fois supérieure aux cellules de testicules adultes non triées. Ensuite, en poursuivant le fractionnement avec GFRA1 et KIT, j'ai constaté que toutes les sous-fractions conservaient une activité SSC in vivo et in vitro, ce qui indique que ni la perte de GFRA1 ni le gain de KIT n'indiquent un appauvrissement en cellules souches. Cependant, la perte de THY1 correspondait à l'épuisement des SSC. De futures études devraient explorer THY1 en tant que marqueur du destin, étant donné que la perte de l'expression de THY1 reflète le plus précisément la sortie de l'état de cellule souche; plus que la perte de GFRA1 ou le gain de KIT. En outre, les sous-fractions GFRA1/KIT peuvent être examinées plus en détail grâce au profilage transcriptionnel, en particulier pour discerner l'identité des cellules GFRA1+ KIT+. Il est important de noter que mon

étude servira de ressource utile pour les futures études sur l'isolement des SSC afin d'obtenir des SSC pures ou presque pures.

Acknowledgements

I would first like to thank my supervisor, Dr. Nagano, for his guidance. It was incredibly fun to get a feel for biological research, something I had no experience in. His strong passion for biology has been inspiring and given me a better appreciation for it. As a trainee, his mentorship over the past two years was extremely valuable. I would like to thank him for all the time and effort he spent on my training.

Thank you to Xiangfan for your endless support and guidance in the lab. I entered my master's degree with no experience working in a biology lab. Xiangfan taught me everything at the lab from the basics. I could not have done it without her. Also, thank you Joelle, for your advice and help in establishing the protocols for my project.

I would like to thank my thesis committee members: Dr. Hugh Clarke, Dr. Jacquetta Trasler, and Dr. Ines Colmegna for their direction and advice throughout my degree.

The members of the Immunophenotyping Platform at the RI (Ekaterina, Hélène, Marie-Helene) were invaluable for their advice in flow cytometry. I would like to thank them for handling FACS sorting. Also, I would like to thank the Molecular Imaging Platform at the RI (Min, Shibo) for their advice on confocal microscopy.

Finally, I would like to thank my parents for their never-ending support.

We acknowledge the support of the Natural Sciences and Engineering Research Council of Canada (NSERC) [Canada Graduate Scholarships - Master's program].

Contributions of Authors

Xiangfan Zhang performed all spermatogonial transplantations, some of which were assisted by Youngmin Song. FACS (fluorescence activated cell sorting) was performed by the RI-MUHC (Research Institute of the McGill University Health Centre) Immunophenotyping Platform. Histological embedding and sectioning following X-gal staining of recipient testes from spermatogonial transplantation was performed by the RI-MUHC Histopathology Platform. The Animal Resources Division at the RI-MUHC helped maintain and provided animal care for experimental mice. Youngmin Song performed all other experiments. Data collection was conducted by Youngmin Song. Data analyses were performed by Youngmin Song with guidance from Dr. Makoto Nagano. Manuscript was written by Youngmin Song with guidance from Dr. Makoto Nagano.

Table of Contents

List of Figures

Figures 7A, 7B, and 8A were created partly with BioRender.com.

List of Tables

List of Abbreviations

BD: Becton, Dickinson and Company

BLIMP1: B Lymphocyte-Induced Maturation Protein 1

BMP: Bone Morphogenetic Protein

BTB: Blood-Testis Barrier

CFA: Cluster Forming Assay

E: Embryonic day (days post-coitum)

EPCAM: Epithelial Cell Adhesion Molecule

EPHA2: Ephrin Receptor A2

ETV5: ETS Variant Transcription Factor 5

FACS: Fluorescence-Activated Cell Sorting

FC: Flow Cytometry

FGF2: Fibroblast Growth Factor 2

FSH: Follicle-Stimulating Hormone

GDNF: Glial Cell Line-Derived Neurotrophic Factor

GFRA1: GDNF Family Receptor Alpha 1

HBSS: Hanks' Balanced Salt Solution

HEPES: N-2-hydroxyethylpiperazine-N-2-ethane sulfonic acid

HSC: Hematopoietic Stem Cell

hSSC: Human Spermatogonial Stem Cell

ID4: Inhibitor of Differentiation 4

ITGA6: Integrin Subunit Alpha 6

ITGB1: Integrin Subunit Beta 1

LIF: Leukemia Inhibitory Factor

MACS: Magnetic-Activated Cell Sorting

MCAM: Melanoma Cell Adhesion Molecule

NANOS2: Nanos C2HC-Type Zinc Finger 2

NANOS3: Nanos C2HC-Type Zinc Finger 3

NEUROG3: Neurogenin 3

P: Postnatal day (days post-partum)

PBS: Phosphate-Buffered Saline

PGC: Primordial Germ Cell

qPCR: Quantitative Real-Time PCR

RA: Retinoic Acid

scRNA-seq: Single-Cell RNA Sequencing

SCF: Stem Cell Factor

SEM: Standard Error of the Mean

SLAM: Signaling Lymphocytic Activation Molecule

SOHLH1: Spermatogenesis and Oogenesis Specific Basic Helix-Loop-Helix 1

SOHLH2: Spermatogenesis and Oogenesis Specific Basic Helix-Loop-Helix 2

SSC: Spermatogonial Stem Cell

STRA8: Stimulated by Retinoic Acid 8

TSPAN8: Tetraspanin 8

Tukey's HSD: Tukey's Honestly Significant Difference Test

X-gal: 5-bromo-4-chloro-3-indolyl β-D-galactoside

ZBTB16: Zinc Finger and BTB Domain Containing 16

1. Introduction

In humans, around a hundred million sperm are produced daily per testis, which is roughly equivalent to five million sperm per hour or one thousand sperm per heartbeat (Amann, 2009). Here, “production” is the creation of daughter cells by spermatogonial stem cells (SSCs), which differentiate and mature into sperm. In essence, SSCs are the driving force behind the highly productive and clockwork-like process of spermatogenesis. While it has been almost 30 years since the development of spermatogonial transplantation to functionally identify SSCs (Brinster and Avarbock, 1994; Brinster and Zimmermann, 1994), their exact identity has yet to be unraveled. All types of studies—from morphological, functional, to transcriptomic studies have not been able to discern a lone, pure SSC population. Elucidating the identity of SSCs in the mouse model will aid in studying human SSCs and attaining their clinical potential in fertility treatments. The fertility preservation of prepubertal boys undergoing gonadotoxic treatments is particularly an important issue, as they cannot produce sperm for sperm banking. In this context, the study of prepubertal mice could be most applicable for fertility treatments, as they are still undergoing development much like prepubertal boys. In my thesis study, I isolated SSCs from prepubertal mice and identified spermatogonial subpopulations that are heterogeneous in stem cell activity. Our work improves on previous purification studies and gleans new insights into spermatogonial commitment during postnatal development. I hope this work will be a springboard for future studies that will isolate pure SSCs, and it will be a useful model for studying human SSCs.

1.1 Spermatogenesis

Spermatogenesis is the process of sperm production in the testes, a highly organized process that is completed with the release of spermatozoa into the lumen of the seminiferous tubules (Clermont, 1972). Spermatogonia are the first of four phases in spermatogenesis: spermatogonia, spermatocyte, spermatid, and spermatozoa, in order of increasing maturity. Spermatogonia are diploid and undergo meiosis at the spermatocyte stage to become haploid gametes (Griswold, 2016). It requires ~68 days

in humans for spermatogonia to complete maturation and be released into the lumen, and ~35 days in mice (Chen et al., 2017; de Rooij, 2017). The layers of spermatogenesis in the seminiferous tubules are spatially organized with the most primitive cells lying along the basement membrane and the most mature cells near the lumen (Fig. 1). Localized together with germ cells, Sertoli cells are a type of somatic cell in the seminiferous tubules (Jégou, 1992). Sertoli cells have important functions in supporting germ cell development, such as cell signaling to germ cells (e.g. GDNF, FGF2, LIF, WNT5A), transduction of endocrine signals (e.g. FSH), and nutrient and waste transport (França et al., 2016; Yeh et al., 2011). Notably, Sertoli cells create a blood-testis barrier (BTB), which segregates the seminiferous epithelium into basal and adluminal compartments (Mruk and Cheng, 2015). Meiotic germ cells past the leptotene stage are located in the adluminal compartment, where they are protected by the immune-privileged microenvironment created by the BTB (Mruk and Cheng, 2015). Spermatogonia and preleptotene spermatocytes are located in the basal compartment, where they are exposed to blood and lymphatic fluid (Mruk and Cheng, 2015). Amazingly, leptotene spermatocytes traverse the BTB through the tight junctions, from the basal to adluminal compartment, and this has been reported to occur through a process of synchronized assembly and disassembly of tight junction proteins (Smith and Braun, 2012).

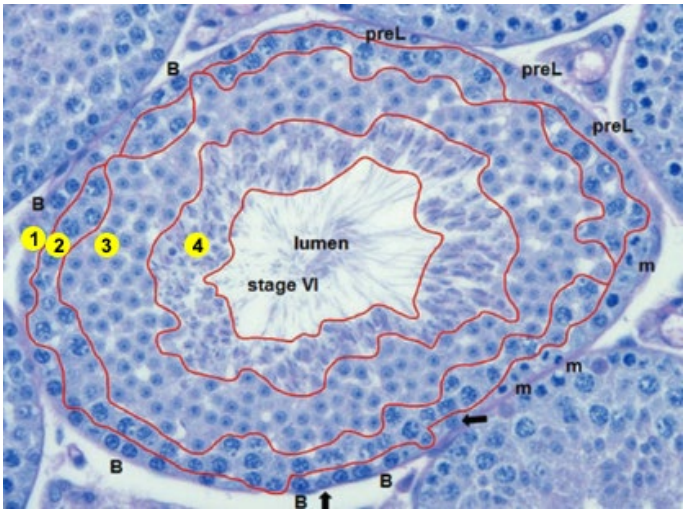

Figure 1. Organization of the seminiferous epithelium. Adapted from de Rooij, 2017. Reproduced with permission from Springer Nature. Cross section of mouse testis. Spermatogonia including SSCs are located in layer 1, along the basement membrane.

1.2 Spermatogonial stem cells

Spermatogenesis is sustained by spermatogonial stem cells (SSCs), a rare cell population estimated to be 0.01% of the adult testis population (Nagano, 2003). By definition, stem cells self-renew as well as produce progenitors that develop into mature differentiated cells (Wagers and Weissman, 2004). They range from totipotent cells that can generate all cells in the body (e.g. mouse embryo until eight-cell stage of morula) (Wobus and Boheler, 2005) to unipotent stem cells like SSCs that produce one mature cell type (sperm). SSCs are also adult stem cells, or tissue-specific stem cells, because their regenerative potential is restricted to one organ, the testis (Wagers and Weissman, 2004). The definition of progenitor is not clearly established, although most definitions will agree that they are more committed than definitive stem cells.

SSCs are unequivocally identified with the spermatogonial transplantation assay, a functional assay in which cells are injected into recipient testes to examine if they can regenerate spermatogenesis (Brinster and Zimmermann, 1994). The assay was published by Ralph L. Brinster's laboratory in 1994 (Brinster and Avarbock, 1994; Brinster and Zimmermann, 1994). In this technique, a transgenic donor strain such as ROSA26-lacZ is often used, which expresses β-galactosidase ubiquitously in all tissues (Friedrich and Soriano, 1991). Thus, donor cells can be identified after transplantation into recipient testes by X-gal staining, which marks them with a blue color (Fig. 2). Recipient mice are typically treated with busulfan to eradicate germ cells, or a strain like W/Wv is used which genetically lacks spermatogenesis. It is important that recipient testes lack germ cells, as the injected donor cells must home to the basement membrane and colonize there. After donor cells are injected, the assay requires 2-3 months of time (2-3 cycles of spermatogenesis) such that SSCs can colonize the basement membrane and proliferate, and its daughter cells can differentiate to form sperm, regenerating spermatogenesis.

The main readout of this assay is the quantity of colonies found in recipient testes, which signify donor-derived spermatogenesis. Importantly, because each SSC colony is formed by a single SSC, it allows for quantification of SSCs based on the number of donor colonies in recipient testes (Kanatsu-Shinohara et al., 2006; Nagano et al., 1999;

Zhang et al., 2003). Thus, blue colonies in the recipient testes can be counted, and using the homing rate/efficiency (the number of colonies in recipient divided by the number of SSCs transplanted) determined in previous studies (Nagano, 2003), the number of SSCs in the original donor cell suspension can be estimated. Overall, the transplantation assay is both the unequivocal assay to confirm SSC identity and to quantify SSCs, and it allows us to estimate SSC enrichment in donor cells (i.e., degree of concentration, or the number of SSCs divided by the number of total cells). While the assay is very powerful, it takes a long time to acquire results (2-3 months) and is a labor-intensive procedure.

A shorter assay that can detect SSC activity is the cluster-forming assay (CFA), requiring only 6-7 days (Yeh et al., 2007). Cells are seeded on top of a STO feeder (embryonic fibroblast) layer and cultured in serum-free mouse SSC culture conditions (Kubota et al., 2004). After a few days, “clusters” or three-dimensional aggregates of spermatogonia appear in culture (Fig. 3). This is indicative of proliferative activity by germ cells, and these clusters can be transplanted to confirm regenerative activity (Yeh et al., 2007). Clusters can be serially passaged every 5-7 days for at least two years (Kanatsu-Shinohara et al., 2005; Kubota et al., 2004).

For the cluster-forming assay (CFA), culture is typically stopped after 6-7 days and clusters are fixed, followed by X-gal staining to visualize testis cells. Finally, clusters are counted; the CFA is a quantitative assay that allows us to estimate the number of cluster-forming cells originally seeded. We can perform this analysis because clusters are clonal (Yeh et al., 2007), indicating that each cluster is formed from one cluster-forming cell. Although a cluster is not definitive evidence of stem cell activity, because spermatogenic differentiation cannot be achieved in vitro, the numbers of clusters in vitro correlates to the number of colonies formed in vivo (SSCs) (Yeh et al., 2007).

In summary, the CFA is a short-term assay that can detect SSCs in vitro, although it is not an unequivocal SSC assay because it does not detect production of terminally differentiated cells (spermatozoa). However, when stem cells are defined by their function to self-renew and produce differentiated cells, continuous production of clusters over a long culture period indicates the presence of long-term self-renewal activity, one

of the two functions that define stem cells. Furthermore, the CFA is much less time-consuming and labor-intensive than the transplantation assay.

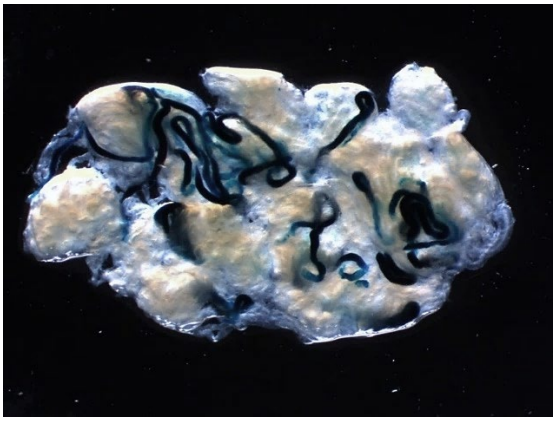

Figure 2. X-gal-stained recipient testis following the transplantation assay. Only donor cells are stained blue. Many SSC colonies can be seen in the recipient testis. ROSA pup testis cells were used as donors.

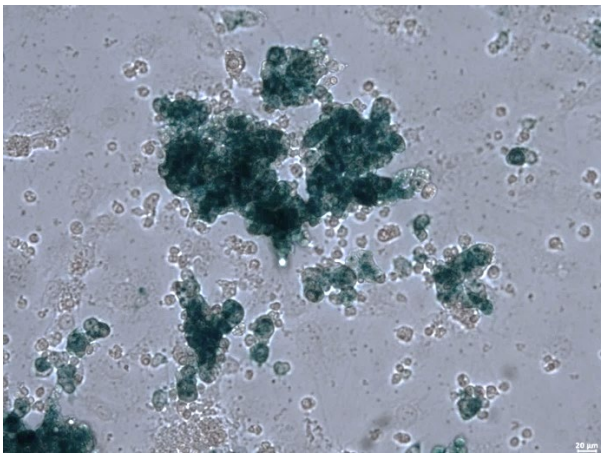

Figure 3. Clusters generated from P9 ROSA pups (after four passages). Cells are blue due to X-gal staining.

1.3 Pre- and Post-natal development of mouse germ cells

The precursor to SSCs is primordial germ cells (PGCs), which derive from the epiblast of the inner cell mass of the blastocyst (Hayashi et al., 2007). In mouse, BLIMP1 is a transcription factor necessary for PGC specification that represses somatic genes, and

a few BLIMP1-expressing cells first appear in the proximal epiblast at ~E6.25 (Saitou and Yamaji, 2012). Extraembryonic factors like BMP4 and BMP8b are also essential to PGC specification (Hayashi et al., 2007). BMP2 from proximal visceral ectoderm (Ying and Zhao, 2001), WNT3 (Ohinata et al., 2009), and SMAD1,2,4,5 (Saitou and Yamaji, 2012) are notable signaling factors involved in PGC fate determination. IFITM3 (Fragilis) and DPPA3 (Stella) are two PGC-specific markers (Saitou et al., 2002) but knockout studies have shown that neither is essential for PGC specification (Richardson and Lehmann, 2010; Saitou and Yamaji, 2012).

IFITM3-expressing cells are first identified in the proximal epiblast at E6.25-6.5, but these are precursors of PGCs that are not yet restricted in lineage to germ cells, producing somatic cells as well (Richardson and Lehmann, 2010; Saitou et al., 2005). Around E7.25, PGCs appear in the posterior extraembryonic mesoderm, and are positive for alkaline phosphatase, IFITM3, DPPA3, and BLIMP1 among many other markers (Richardson and Lehmann, 2010; Saitou et al., 2005; Saitou and Yamaji, 2012). They then migrate through hindgut endoderm and mesoderm, arriving at the genital ridges at E10.5-11.5 (Richardson and Lehmann, 2010). PGCs initiate mitotic arrest in males by E13.5 (Western et al., 2008), whereas in females they begin to undergo meiosis by E13.5 (Speed, 1982). Male PGCs from E8.5-16.5 can regenerate spermatogenesis upon transplantation, indicating SSC function, and these sperm can produce offspring with microinsemination (Chuma et al., 2005). However, PGCs up to E12.5 also produce teratomas when transplanted, indicating differentiation into other lineages, and are not very efficient at regenerating spermatogenesis (Chuma et al., 2005). PGCs from E14.5 and later show relatively efficient regeneration of spermatogenesis without teratoma formation (Chuma et al., 2005; Ohta et al., 2004).

After initiating mitotic arrest by E13.5 (Western et al., 2008), male germ cells stay quiescent until ~P2 (Culty, 2009; Vergouwen et al., 1991). The germ cells during this period are called “gonocytes” or “prospermatogonia” and I will refer to them as the latter. Notably, male germ cells undergo genome-wide DNA demethylation from E10.5-12.5 (Hajkova et al., 2002), and after becoming quiescent, acquire paternal methylation imprints (Sasaki and Matsui, 2008). At birth, prospermatogonia are located in the lumen

of seminiferous tubules. They migrate to the basement membrane, begin proliferating by P3-4, and are then referred to as spermatogonia (Geyer, 2017). Prospermatogonia can be further divided into quiescent T_1-prospermatogonia (E15 to P2) and dividing T_2-prospermatogonia (P2 to P3) (McCarrey, 2017).

In my study, I focused on three stages of postnatal development: P0-2, P8-9, and P16-18. Germ cells at P0-2 are quiescent prospermatogonia in the lumen. By P3-4, they have started proliferating, at which point they are called spermatogonia (or more specifically, type A spermatogonia) and can be morphologically classified into A_{single}, A_{pair}, A_{al}, and A_{1-4} spermatogonia (Geyer, 2017; Huckins and Oakberg, 1978). Notably, the spermatogonial population at this point is incredibly heterogeneous at both the protein and transcript levels (Green et al., 2018; Hermann et al., 2015; Law et al., 2019; Niedenberger et al., 2015; Suzuki et al., 2009; Tan et al., 2020). The first cells starting to undergo meiosis, or preleptotene spermatocytes, appear by P8-10 (Bellve et al., 1977; Geyer, 2017; Yoshinaga et al., 1991). Sertoli cells stop proliferating at P14-17 (Vergouwen et al., 1991; Walker, 2003) and the BTB forms by P15 (Chihara et al., 2013; Willems et al., 2010). By P16-18, the number of germ cells have increased significantly compared to earlier ages. This increase continues as the first wave of spermatogenesis completes around P30-35 and the first spermatozoa are released (Janca et al., 1986).

1.4 The first wave of spermatogenesis

The first wave of spermatogenesis is distinct from all subsequent waves of spermatogenesis, which are collectively referred to as adult “steady-state” spermatogenesis (Geyer, 2017; McCarrey, 2017). Germ cells during the first wave can be subdivided into committed progenitors that undergo meiosis to form the first sperm and the newly established SSC population which develops and expands as it matures into the “adult” SSC pool. The first wave is unique in that committed progenitors are not derived from the SSC population; the SSC population is established at some point after P2, while a committed progenitor population seems to already exist beforehand.

Several mutant mouse strains (e.g. *jsd* (Beamer et al., 1988), *Rb1* (Hu et al., 2013), and *Zbtb16* (Costoya et al., 2004)) show successful spermatogenesis in the first wave followed by gradual disruption of spermatogenesis over time, leading to infertility as an adult. These results imply that the first wave has different properties when compared to subsequent waves of spermatogenesis, which may be due to developing germ cells and soma (including the neuroendocrine system). Thus, there is ample reason to examine the first wave of spermatogenesis by itself.

It is argued that the first sperm do not originate from SSCs but progenitors that lost long-term self-renewal capacity and thus, the first wave is SSC-independent while the subsequent waves are SSC-dependent (Geyer, 2017; Hermann et al., 2018; Tan et al., 2020). Equivalently, the prospermatogonial population can be separated into one population that differentiates into the first wave and another that forms the SSC pool (de Rooij, 1998; Law et al., 2019; Tan et al., 2020; Velte et al., 2019; Yoshida et al., 2006).

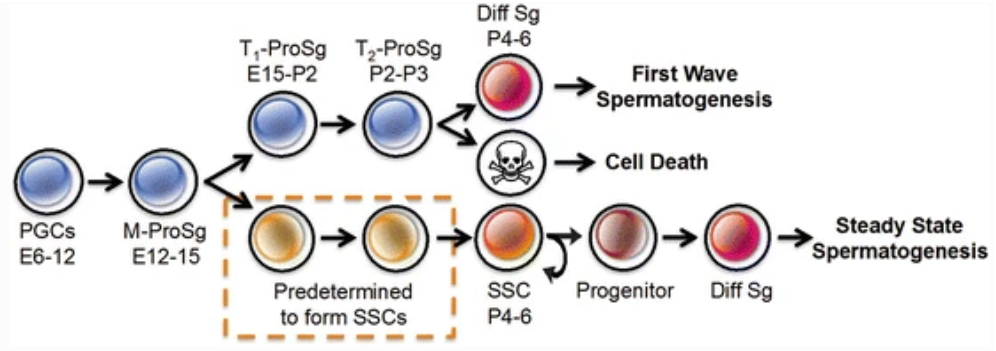

Figure 4. Scheme of two distinct prospermatogonial populations in mouse. Adapted from McCarrey, 2017. Reproduced with permission from Springer Nature. This figure suggests that SSCs are predetermined by E15.

Previous studies have found that the functional activity of prepubertal germ cells is different from that of steady-state germ cells. As for the first-wave progenitors that form the first sperm, they undergo increased apoptosis (Mori et al., 1997), a faster rate of maturation (Kluin et al., 1982), and reduced efficiency in fertilization (Miki et al., 2004). As for prepubertal SSCs, they seem to divide at a higher frequency, shown by higher rates of retroviral integration (Nagano et al., 2002b, 2001). Also, prepubertal SSCs may

be geared more towards differentiation rather than self-renewal when compared to steady-state SSCs (Ebata et al., 2007). However, they are not less capable than adult SSCs, because they are capable of complete regeneration of spermatogenesis and exhibit a similar homing efficiency as adult SSCs (Ebata et al., 2007).

1.5 Heterogeneity of prepubertal spermatogonia

Prepubertal spermatogonial populations are heterogeneous and can be subdivided both at the protein and transcript level. Be cautioned that expression at the protein and transcript levels can be different, as markers like KIT, STRA8, and SOHLH2 are not uniformly expressed in spermatogonia at the protein and transcript levels (Hermann et al., 2015). Immunofluorescence studies show subpopulations with distinct protein expression as early as P4, with there being 60% GFRA1+ KIT–, 35% GFRA1– KIT+, and less than 10% GFRA1+ KIT+ spermatogonia (Niedenberger et al., 2015). Single-cell RNA sequencing studies have elucidated the subpopulations in greater resolution. Increasing heterogeneity perinatally is shown from one scRNAseq cluster/population at E18.5, to two populations at P2, and finally three populations at P7 (Tan et al., 2020). That being said, one study has found heterogeneity from E16.5 in terms of ID4 expression (Law et al., 2019).

Undifferentiated spermatogonia of prepubertal mice can be further subdivided, often into one population that is more naïve and another that is more “progenitor-like” (Hermann et al., 2018; Tan et al., 2020). Consensus SSC genes from scRNA-seq studies include *Gfra1*, *Id4*, *Etv5*, *Lhx1*, *Eomes*, *Dusp6*, and *Ret* while consensus “progenitor” and differentiation genes include *Sohlh1*, *Nanos3*, *Dmrt1*, *Ngn3*, *Rarg*, *Stra8*, and *Kit* (Green et al., 2018; Hermann et al., 2018; Law et al., 2019; Liao et al., 2019; Tan et al., 2020). While it can be difficult to compile the vast amount of information from all scRNA-seq studies, I will summarize a few key points here. First, they have identified cell clusters/populations with distinct gene expression profiles at various points in prepubertal development, from as early as P2 (Law et al., 2019; Tan and Wilkinson, 2020). Second, new markers like CD87 (Liao et al., 2019) and CD82 (Tan et al., 2020) have emerged from scRNA-seq studies as potential SSC surface markers. Third,

intracellular signaling pathways involved in SSC establishment have been examined, such as the Hippo (Tan et al., 2020), mTORC1 (Suzuki et al., 2021), eIF2 (Hermann et al., 2018; Tan et al., 2020), and MAPK pathways (La et al., 2018; Tan et al., 2020). While scRNA-seq studies have not been able to elucidate the SSC population definitively, they have and will continue to be a useful resource in characterizing heterogeneous cell populations. Future studies could attempt multi-omics approaches to elucidate spermatogonial subpopulations, including proteomics, epigenomics, and metabolomics analyses.

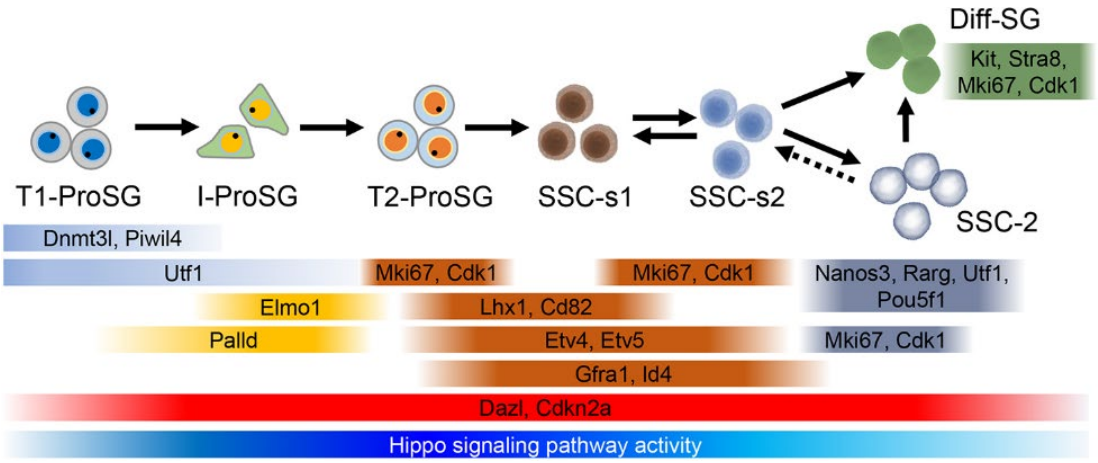

Figure 5. Expression of genes in SSC development as revealed by scRNA-seq. Adapted from Tan et al., 2020. Prospermatogonia are divided into three separate phases: T_1-Prospermatogonia, I-Prospermatogonia, and T_2-Prospermatogonia. *Gfra1*, *Id4*, *Etv5*, *Nanos3*, *Stra8*, and *Kit* are markers that I examined in my study. Reproduced with permission (Development, The Company of Biologists).

1.6 Surface markers used for spermatogonial fractionation

More than a dozen markers have been reported for use in the fractionation of spermatogonia with FACS or MACS. Some notable markers are listed in the table below. I will provide brief statements about the characteristics of each marker molecule. Only studies in mouse were selected.

+ Marker	Reference	**- Marker**	Reference
ITGA6	(Shinohara et al., 1999)	KIT	(Shinohara et al., 2000)
ITGB1	(Shinohara et al., 1999)	ITGAV	(Shinohara et al., 2000)

THY1	(Kubota et al., 2003)	MHC-I	(Kubota et al., 2003)
CD9	(Kanatsu-Shinohara et al., 2004)	EPCAM	(Kanatsu-Shinohara et al., 2011)
GFRA1	(Ebata et al., 2005)		
CDH1	(Tokuda et al., 2007)		
MCAM	(Kanatsu-Shinohara et al., 2012)		
TSPAN8	(Mutoji et al., 2016)		
EPHA2	(Morimoto et al., 2020)		

Table 1. List of positive and negative SSC surface markers previously used in FACS or MACS.

ITGA6

Integrin Subunit Alpha 6 is one of 18 integrin alpha subunits (Campbell and Humphries, 2011). Integrins are heterodimers of alpha and beta subunits, and are surface proteins involved in signaling pathways and tissue organization (Campbell and Humphries, 2011). In particular, integrin α6 (ITGA6) and integrin β1 (ITGB1) are known to bind laminin and collagen, components of the extracellular matrix and basement membrane (Campbell and Humphries, 2011; Shinohara et al., 2000). They were identified as SSC markers in mice based on attachment to these extracellular matrix molecules (laminin, collagen IV, fibronectin) (Shinohara et al., 1999). Selection of cells attaching to laminin molecules led to a significant enrichment of SSCs but not collagen IV or fibronectin, as measured by spermatogonial transplantation (Shinohara et al., 1999). Both ITGA6 and ITGB1 lead to significant SSC enrichment when used independently as single markers in MACS (Shinohara et al., 1999). Finally, ITGA6 has been used for human SSC enrichment as well (Givelet et al., 2022; Nickkholgh et al., 2014; Valli et al., 2014).

THY1

THY1 or CD90 is a glycosylphosphatidylinositol-anchored (GPI-anchored) surface protein that is expressed in a large variety of cells including thymocytes, neurons, fibroblasts, mesenchymal stem cells, hematopoietic stem cells, embryonic stem cells, and SSCs (Draper et al., 2002; Kubota et al., 2003; Kumar et al., 2016). THY1 was identified as a SSC marker based on spermatogonial transplantation experiments

(Kubota et al., 2003) and is used as a positive marker to enrich mouse SSCs with MACS for in vitro culture (Kubota et al., 2004). In mice, THY1+ cells could not be visualized by immunostaining before my thesis study, and were detectable so far only by flow cytometry, making it difficult to characterize THY1+ cells. THY1 is an efficient mouse SSC marker, providing the highest enrichment across markers when they are used in single-antigen cell sorting experiments (Kubota et al., 2003).

The function of THY1 in SSCs is unknown. In other cell types, THY1 functions as a cell adhesion molecule and interacts with integrins and syndecans (Avalos et al., 2009; Fiore et al., 2014). For example, in endothelial cells, THY1 is suggested to mediate leukocyte adhesion to the endothelium by interacting with integrin αMβ2 on leukocytes (Wetzel et al., 2004). In addition, THY1 on endothelial cells interacts with integrin αvβ3 on melanoma cells to mediate adhesion to the endothelium (Saalbach et al., 2005). THY1 contains an RGD motif (tripeptide Arg-Gly-Asp, or Arginine-Glycine-Aspartic Acid), which is recognized by integrins and mediates binding to integrin proteins (D'Souza et al., 1991; Leyton et al., 2001; Main et al., 1992). Interaction between THY1 on neurons and integrin β3 on astrocytes, which is important for astrocyte function, can be blocked with RGD-related peptides (Kong et al., 2013; Leyton et al., 2001). In summary, THY1 in endothelial cells and neuronal cells acts as an adhesion molecule and binds to integrins. Because integrin α6 and integrin β1 and are both expressed on SSCs (Shinohara et al., 1999), I speculate that THY1-integrin binding may also occur in germ cells.

Interestingly, THY1-knockout mice are fertile, implying THY1 function is nonessential in spermatogenesis (Barlow et al., 2002; Nosten-Bertrand et al., 1996).

GFRA1

Glial cell line-derived neurotrophic factor (GDNF) receptor alpha 1 is another GPI anchored surface protein that is a receptor for both GDNF and neurturin (Cacalano et al., 1998). GDNF binding to GFRA1 leads to recruitment of the receptor tyrosine kinase RET and formation of the GDNF-GFRA1-RET complex, followed by

autophosphorylation of RET and intracellular signal transduction (Kawai and Takahashi, 2020). The GDNF signaling pathway promotes SSC self-renewal (Chen et al., 2016; Sharma and Braun, 2018; Takashima et al., 2015) and GDNF is a potent proliferation factor for SSCs in vitro (Kubota et al., 2004). In adult mice, immunostaining studies showed that GFRA1 expression is limited to undifferentiated Type A spermatogonia and expression is highest in A_{single} spermatogonia, which is the most primitive stage of spermatogonia that can be morphologically classified (Grasso et al., 2012; Grisanti et al., 2009; Nakagawa et al., 2010). However, GFRA1 expression is heterogeneous even among the morphologically most primitive spermatogonia, A_{single} spermatogonia (Grasso et al., 2012; Grisanti et al., 2009; Nakagawa et al., 2010). The enrichment of mouse SSCs with GFRA1 has seen mixed success, although more successful in FACS purification than MACS (Buageaw et al., 2005; Ebata et al., 2005; Garbuzov et al., 2018; Grisanti et al., 2009; Takashima et al., 2015).

KIT

Proto-oncogene *kit* is a receptor tyrosine kinase and the homolog of the viral oncogene *v-kit* of the HZ4 feline sarcoma virus (Yarden et al., 1987). KIT (or mast/stem cell growth factor receptor) is essential in melanocyte development (Wehrle-Haller, 2003), expressed on hematopoietic stem cells (HSCs), and is required for hematopoiesis and spermatogenesis (Mintz and Russell, 1957). KIT ligand or stem cell factor (SCF), produced by Sertoli cells in the testis, is a ligand for KIT, and SCF production by Sertoli cells is essential in maintaining spermatogenesis (Peng et al., 2023; Strohmeyer et al., 1995).

Regarding the function of KIT in spermatogenesis, it is essential in spermatogonial differentiation (Schrans-Stassen et al., 1999; Yoshinaga et al., 1991). Studies report that KIT expression is limited to differentiating spermatogonia and preleptotene spermatocytes, and not expressed in late spermatocytes or spermatids (Yoshinaga et al., 1991). Notably, blocking KIT causes depletion of differentiating spermatogonia and later stages of germ cells, but undifferentiated Type A spermatogonia continue to survive and proliferate (Ohta et al., 2003; Yoshinaga et al., 1991).

Undifferentiated Type A spermatogonia in adults have been observed to not express KIT, based on immunofluorescence studies (Yoshinaga et al., 1991). However, there was a report of undifferentiated spermatogonia in prepubertal pups (P7.5) expressing KIT (Ohbo et al., 2003). Furthermore, KIT+ cells in vivo retain some SSC activity, although activity is generally lower than KIT– cells (Barroca et al., 2009; Kanatsu-Shinohara et al., 2012; Ohbo et al., 2003; Shinohara et al., 2000). One study actually found higher SSC enrichment in KIT+ cells than unsorted control (bulk adult testis cells) (Shinohara et al., 1999).

KIT is commonly used as a negative marker in mouse SSC enrichment. KIT is expressed in cultured SSCs in vitro and there is no difference between KIT+ and KIT– cells in regenerative activity (Morimoto et al., 2009). Interestingly, KIT is expressed in PGCs, as well as in oocytes, zygotes (Motro and Bernstein, 1993), inner cell mass of blastocysts, and embryonic stem cells (Bashamboo et al., 2006). This protein plays an important role in the development of these cell types (Zhao and Garbers, 2002). Prospermatogonia at birth do not express KIT (Niedenberger et al., 2015; Yoshinaga et al., 1991) but its expression has been reported to reappear in spermatogonia by P3.5-4 (Niedenberger et al., 2015; Ohbo et al., 2003).

1.7 Summary

Safeguarding the fertility of prepubertal boys undergoing gonadoxic treatments (e.g. radiotherapy, chemotherapy), who cannot produce sperm for sperm banking, could be attained in the future through SSC research. An important requirement that must be met is the establishment of human (h)SSC isolation and hSSC in vitro expansion. At the isolation step, an efficient purification of hSSCs is necessary. While many efforts have been made in this regard (Givelet et al., 2022; He et al., 2012; Liu et al., 2011; Zohni et al., 2012), it is difficult to assess the efficiency of purification because validating regeneration activity of hSSCs with the transplantation assay is not feasible in humans. Xenotransplantation of human spermatogonia into mouse can lead to long-term survival but they do not regenerate spermatogenesis (Nagano et al., 2002a; Wyns et al., 2008), while transplantation in human recipients for experimental purposes is unethical. As for

the in vitro expansion of hSSCs, long-term culture attempts have generally been unsuccessful, with insufficient proliferation of hSSCs and length of culture period (Lim et al., 2010; Medrano et al., 2016; Zheng et al., 2014). Perhaps human scRNA-seq studies will identify factors that can improve hSSC culture attempts (Guo et al., 2017; Shami et al., 2020; Sohni et al., 2019), such as by finding signaling pathways upregulated in hSSCs and ligand-receptor interactions between somatic cells and hSSCs. In summary, the study of hSSCs has been limited due to the lack of assays to validate stem cell activity.

In mice, lone SSCs may be close to being identified. Unpublished results from our lab show that SSCs in adult mice can be isolated at a purity of ~1 in 10 cells. SSC isolation has improved significantly in the past two decades. Initially, induction of cryptorchid testes was used to achieve high SSC enrichment (Shinohara et al., 2000). Induction of experimental cryptorchidism, by suturing mouse testes to the abdominal wall, destroys endogenous spermatogenesis and eliminates the majority of germ cells due to exposure to a high body core temperature. Since SSCs survive these conditions, the cells can be enriched in vivo in cryptorchid testes. Currently, however, the best methods are cell fractionation using FACS in intact testes or transgenic reporters, particularly ID4 (inhibitor of DNA binding 4) (Chan et al., 2014). ID4-EGFP+ cells (from *Id4-eGfp* transgenic reporter mice) have often been used as an SSC population for scRNA-seq studies and P8 ID4-EGFP^{Bright} cells show high SSC activity (~180 colonies / 10^5 cells transplanted) in the transplantation assay (Helsel et al., 2017). But for the enrichment or purification of hSSCs, such use of a transgenic reporter is not translatable to humans. Therefore, isolation and purification of hSSCs must be done with FACS using endogenous cell-surface markers in intact cells without genetic markers.

In this study, I extensively fractionated spermatogonia populations at three points in prepubertal development (P0-2, P8-9, P16-18) with FACS and examined all relevant subpopulations. Prepubertal SSCs are the focus in the clinical translation of SSC research, and the first wave of spermatogenesis is unique, prompting separate study of these cells. This study examines SSC development in the mouse model and could serve as a preclinical model for prepubertal hSSCs.

In the subpopulations I identified, SSC activity was examined both in vivo with the transplantation assay and in vitro with the cluster forming assay (CFA) (Yeh et al., 2007). Our work catalogs the spermatogonial subpopulations throughout development and tracks the SSC immunophenotype in terms of four surface markers: THY1, ITGA6, GFRA1, and KIT. By providing detailed cell characteristics, this work lays a foundation for the extensive FACS purification of SSCs and gives an extensive resource for the study of SSCs in other mammalian species, including human.

2. Methods

2.1 Spermatogonial transplantation

ROSA26 mice (B6;129S-Gt(ROSA)26Sor/J) were used in all experiments, which express β-galactosidase ubiquitously in all tissue including testis (Friedrich and Soriano, 1991). For spermatogonial transplantation, 129/SvEv × C57BL/6 F1 hybrid mice were used as recipients. Four to eight weeks prior to transplantation, recipient mice were intraperitoneally injected with busulfan (50 mg/kg of body weight) to eliminate endogenous germ cells. Recipient mice underwent busulfan treatment at 4-5 weeks of age. A microinjection needle filled with a single cell suspension of donor cells was inserted into the efferent ducts, and donor cells were injected into the lumen of the seminiferous tubules through the rete testis. Testes of recipient mice were recovered 2-3 months after transplantation and stained with X-gal, or 5-bromo-4-chloro-3-indolyl β-D-galactoside (BioBasic #BB0083) to visualize donor cells.

2.2 Cell culture and the cluster forming assay (CFA)

SSC culture was maintained in a manner similar to previous studies (Kubota et al., 2004; Yeh et al., 2007): a serum-free medium composed of Minimum Essential Medium α (Invitrogen #12561) with 0.2% BSA (Sigma #A3803), 5 μg/mL insulin (Sigma #I5500), 10 μg/mL iron-saturated transferrin (Sigma #T1283), 3 x 10^{-8} M sodium selenite (Sigma #S5261), 50 μM 2-mercaptoethanol (Sigma #M7522), 10 mM HEPES (Sigma #H0887),

60 μM putrescine (Sigma #P5780), 2 mM glutamine (Invitrogen #25030-081), 50 units/mL penicillin and streptomycin (Invitrogen #15070-063), and 7.6 μ eq/L free fatty acids (31 mM palmitic acid (Sigma #P0500), 2.8 mM palmitoleic acid (Sigma #P9417), 11.6 mM stearic acid (Sigma #S4751), 13.4 mM oleic acid (Sigma #O1008), 35.6 mM linoleic acid (Sigma #L1012), 5.6 mM linolenic acid (Sigma #L2376)) (Kubota et al., 2004). The following growth factors were added to culture medium, identical to previous studies (Kubota et al., 2004): recombinant human GDNF (R & D Systems #212-GD), recombinant rat GFRA1 (R & D Systems #560-GR), and recombinant human FGF2 (ThermoFisher #13256-029). For the initial one or two passages, in which the culture is being established, 40 ng/mL GDNF, 300 ng/mL GFRA1, and 1 ng/mL FGF2 were added to culture medium. In subsequent passages, growth factor concentrations were reduced (except FGF2) to 20 ng/mL GDNF, 75 ng/mL GFRA1, and 1 ng/mL FGF2. Culture medium was replaced with fresh medium and growth factors every 3-4 days and cells were treated with 0.25% trypsin-EDTA (Invitrogen #25200-056) for ~3 min. to dissociate them before subculturing.

SSCs were cultured on a layer of STO (SIM mouse embryo-derived thioguanine and ouabain resistant) fibroblasts (Nagano et al., 2003) which were mitotically inactivated with mitomycin C (Sigma # M0503) treatment (10 μg/ml for 3-3.5 hours). STO feeders were seeded in culture plates at 5×10^4 cells/cm^2 at least one day before cluster seeding. Both STO feeders and SSC culture were maintained in 5% CO2 at 37˚C.

The cluster forming assay (CFA) (Yeh et al., 2007) was 6-7 days or 9-11 days in duration depending on the type of experiment. I did not passage cluster cultures in this assay procedure. All CFAs were conducted using 48-well plates. Clusters are defined as three dimensional structures formed with at least six cells, as described in (Yeh et al., 2007). I excluded chain-like structures indicative of spermatogonial differentiation in counting clusters (La et al., 2018). To visualize clusters, wells were fixed with 0.5% glutaraldehyde for at least 5 min., followed by staining with X-gal. Clusters were quantified visually under a light microscope. If clusters were too numerous to manually quantify, the entire well was imaged first, followed by manual quantification.

For counting clusters during long-term culture experiments, cluster numbers were estimated by counting five different locations in a culture well with a light microscope. The average number of clusters per “location” and the field of view (2.2 mm) was used to calculate the total number of clusters per well. Then, previous passage ratios were used to estimate the rate of expansion.

2.3 Flow cytometry (FC) and fluorescence activated cell sorting (FACS)

Below is a concise version of protocols for FC and FACS. An extended protocol, including protocol for intracellular FC, can be found in Appendix 6.2.

After recovering mouse testes, tunica was removed and seminiferous tubules were lightly loosened with forceps. The tubules were digested in Hanks’ Balanced Salt Solution with 1 mg/mL Collagenase I (Sigma #C0130) and 1 mg/mL Collagenase IV (Sigma #C5138) for 10-12 min. at 37°C. PBS was added to the collagenase digestion solution at the end of incubation to dilute the solution. Tubules were sedimented with unit gravity for 10 min. for P8-9 or P16-18 pup testes (see later for P0-2). Supernatant was removed and fresh PBS was added to sediment tubules again for 10 min. This process washed off collagenase while removing a large portion of interstitial cells. For P0-2 pup testes, centrifugation at 500 x *g* for 5 min. was used instead of a unit gravity sedimentation. This is because seminiferous tubules at this developmental stage are so light that unit gravity sedimentation is impractical. Supernatant was removed after centrifugation. Washing was done by adding PBS and centrifuging again at the same settings. To digest tubules to a single-cell suspension, 2-3 mL of enzyme-free cell dissociation buffer (Sigma #S-014-B) was added and incubated for at least 2 min. in a 37°C water bath (volume of dissociation buffer added depends on the amount of tubules being digested). In order to untangle cell clumps that occur due to DNA leakage from dead cells during the digestion procedure, a solution of 5 mg/mL DNase I (Sigma #DN25) was added to give a final concentration of 1 mg/mL DNase I. Once cell clumps were not visible, 7 mL PBS was added to the digestion solution. The resulting cell solution was treated through a 40 µm cell strainer to remove undigested tissue debris.

Cells were stained with a viability dye (Biogems Viability Dye 506) to exclude dead cells. For incubation in primary antibodies, cells were resuspended in PBS with 1% BSA (Sigma #A3803). Antibodies used are detailed in Table 2. Up to 2 x 10^6 cells were resuspended in 100 µL solution

of 1% BSA (PBS) per tube. Cells were incubated in antibody solution for 25-35 min. on ice with a gentle agitation. After incubation, 1 mL of PBS was added into each tube to wash cells, followed by centrifugation of tubes at 500 x *g* for 5 min. Finally, supernatant was removed, and cells were resuspended in 1% BSA in PBS at 200-300 µL per 10^6 cells. For flow cytometry, cells were read on the BD (Becton, Dickinson and Company) LSRFortessa or LSRFortessa X-20. For FACS, cells were sorted on the BD FACSAria Fusion.

Data were analyzed with FlowJo™ v10.7 or v10.8 Software (BD Life Sciences). Below is a table detailing the setup of flow cytometric instruments. For the flow cytometric analyses of clusters, data of all cells after exclusion of doublets and dead cells were used for generating profiles.

BD LSRFortessa/LSRFortessa X-20/FACSAria Fusion								
Laser line	405nm	405nm	405nm	488nm	488nm	561nm	640nm	640nm
Emission filter	710/50	525/50	450/50	530/30	530/30	582/15	780/60	670/14
Fluorochrome	BV711	Biogems 506	BV421	FITC	Alexa Fluor 488	PE	APC-Cy7	APC
Antigen	MHC-I	Viability	KIT	CD45	CD74	THY1	ITGA6	GFRA1

Table 2. Configuration of FC and FACS machines.

2.4 Intracellular flow cytometry

First, surface staining was performed as detailed in section 2.3. After surface staining was complete (including one wash with PBS), cells were fixed in ice-cold 4% paraformaldehyde solution, then incubated for 15 min. on ice with agitation. Cells were washed once with PBS by centrifuging cells at 500 x *g* for 5 min., removing supernatant, and adding 1 mL PBS. Cells were centrifuged again at 500 x *g* for 5 min. and supernatant was removed. In order to permeabilize the cells, they were resuspended in ice-cold 0.1% Triton X-100, followed by incubation for 5 min. on ice. After incubation, cells were centrifuged at 500 x *g* for 5 min., supernatant was removed, and 1 mL PBS was added to wash. Supernatant was removed, then cells were resuspended in blocking buffer (1% BSA in PBS) and incubated for 5 min on ice.

After the blocking process, testes were distributed into sample tubes (1.5 mL Eppendorf) as necessary (e.g. 3 tubes, one for TRA98 and Vimentin staining, one for TRA98 and PLZF staining, and one control). Then, sample tubes were centrifuged at 500 x *g* for 5 min.,

supernatant was removed, and cells were resuspended in 1% BSA (PBS) with primary antibodies (100 uL total volume / tube). The sample tubes were incubated 20 min. on ice with agitation. After incubation was complete, 1 mL PBS was added in each tube to wash, and tubes were centrifuged at 500 x *g* for 5 min., followed by removal of supernatant. Then, cells were suspended in 1% BSA (PBS) with secondary antibodies (100 uL total volume / tube). Sample tubes were incubated 10 min. on ice with agitation. After incubation, 1 mL PBS was added in each tube to wash, followed by centrifugation at 500 x *g* for 5 min. and removal of supernatant. Cells were resuspended in 1% BSA (PBS) solution, 200-300 µL volume per tube, and analyzed on the BD LSRFortessa.

2.5 Antibodies used

The table below details all primary antibodies used in this study. All primary antibodies used for flow cytometry or FACS were directly conjugated to fluorochromes.

Antigen	Fluorochrome	Vendor	Catalog #	Stock conc.	Working conc.	Application
THY1	PE	Biolegend	105308	0.2 mg/mL	1:200	Flow
ITGA6	APC-CY7	Biolegend	313628	0.1 mg/ml	1:200	Flow
GFRA1	APC	R&D	MAB560	1 mg/mL	1:200	Flow
KIT	BV421	Biolegend	105827	0.05 mg/mL	1:333	Flow
MHC-I (H-2K^{b}/H-2D^{b})	BV711	BD	745433	0.2 mg/mL	1:333	Flow
CD45	FITC	Invitrogen	11-0452-82	0.5 mg/mL	1:333	Flow
CD74	Alexa Fluor 488	Biolegend	151006	0.5 mg/mL	1:100	Flow
TRA98	N/A	B-Bridge	73-003	1 mg/mL	1:200	Intra. Flow
THY1	N/A	BD	553000	0.5 mg/ml	1:50	WM IF

The GFRA1 antibody was conjugated to a fluorochrome at my laboratory using the Abcam Lightning-Link APC conjugation kit (ab201807). Instead of the minimum incubation period of 3 hours, I recommend overnight incubation as I found it results in better conjugation (i.e. higher fluorescence intensity). The manufacturer protocol recommends incubation for at least 3 hours, and it states that overnight incubation is suitable.

Viability Dye 506 was from BioGems (Catalog # 62210-00). I used 1 uL antibody for 1 mL cell suspension (up to 10 x 10^6 cells).

For intracellular flow cytometry and whole-mount immunofluorescence, 1:500 Donkey anti-Rat IgG (H+L) Highly Cross-Adsorbed Secondary Antibody, Alexa Fluor 488 (Invitrogen, #A21208, stock concentration 2 mg/mL) was used.

2.6 Whole-mount immunofluorescence (WM IF)

Mouse testes were placed in a petri dish filled with PBS (7 mL) and tunica was removed from testes, while trying not to disturb the structure of the seminiferous tubules. Testes were briefly digested in Hanks' Balanced Salt Solution with 1 mg/mL Collagenase I (Sigma #C0130) and 1 mg/mL Collagenase IV (Sigma #C5138) for ~5 min. at RT (room temperature), with gentle agitation. Tubules were allowed to sediment at unit gravity (< 1 min.), and supernatant was removed as much as possible without removing tubules. PBS (7 mL) was added to wash the tubules, and tubules were allowed to sediment, followed by removal of supernatant. This process was repeated two more times for a total of three washes. Some of the interstitial cells of the testes should be removed after this repeated sedimentation and washing process.

To fix the tubules, 4% paraformaldehyde solution (PBS) was added, enough to fully submerge the testes and more (3 mL). The testes were incubated for 90 min. at 4°C with agitation. Afterwards, the tubules were sedimented at unit gravity (< 1 min.) and supernatant was removed as much as possible without removing tubules. PBS (7 mL) was added to wash the tubules, and tubules were allowed to sediment, followed by removal of supernatant. This process was repeated two more times for a total of three washes. Blocking buffer (1% BSA + 3% Donkey serum in PBS) was added to cells and they were incubated for 30+ min. at RT with agitation. There should be enough volume of blocking buffer such that the testes are fully submerged while being agitated during incubation. After the blocking process, testes were distributed into sample tubes (1.5 mL Eppendorf) as necessary (e.g. 3 tubes, one for THY1 and GFRA1 staining, one for THY1 and KIT staining, and one control). Supernatant was removed until 200 uL solution was remaining, and primary antibodies were added to the solution. Sample tubes were incubated overnight at 4°C with agitation, ensuring that the testes were submerged in solution while being agitated.

The next day, incubation of primary antibodies was stopped by allowing tubules to sediment (< 1 min.), and supernatant was removed as much as possible without removing tubules. PBS (7 mL) was added to wash the tubules, and tubules were allowed to sediment, followed by removal of supernatant. This process was repeated two more times for a total of three washes. In each tube, blocking buffer (1% BSA + 3% Donkey serum in 200 uL PBS) was added with secondary antibodies and Hoechst 33342 to stain nuclei. Sample tubes were incubated in secondary antibody for 2 hours RT with agitation, assuring that testes were submerged in solution during agitation. After incubation was complete, tubules were allowed to sediment, supernatant was removed, and ddH2O (double-distilled or MilliQ) was added to wash. Once again, tubules were allowed to sediment and supernatant was removed. This process was repeated two more times for a total of three washes.

Finally, seminiferous tubules were transferred to glass microscope slides. This can be achieved by using a 1 mL pipette tip that has been cut at the end with scissors to widen the opening. The solution with tubules was pipetted onto a glass slide. Then, forceps were used to manipulate the tubules such that they were reasonably dispersed, and kimwipes were used to remove excess liquid. A drop of mounting medium was added and a cover slip was put over the tubules. The staining procedure was complete, and the tubules were visualized with a microscope.

2.7 Quantitative real-time PCR (RT-qPCR)

The PicoPure RNA isolation kit (ThermoFisher #KIT0204) was used to extract and isolate RNA from cells following FACS. Contaminating DNA was removed by using the RNase-Free DNase set (Qiagen, #79254). Isolated RNA was evaluated for quality and RNA concentration using the NanoDrop 2000 spectrophotometer (ThermoFisher) and 25 ng of starting RNA was used for each sample. Complementary DNA (cDNA) was synthesized with Superscript III Reverse Transcriptase (Invitrogen #18080044), Anchored Oligo dT Primers (Thermofisher #AB-1247), and RNaseOUT (Thermofisher #10777-019). Quantitative PCR was performed on the Roche LightCycler 96 and associated software was used for data analysis. The BlasTaq 2X qPCR MasterMix (abm # G891) was used in amplification. Cycling settings were 3 min. preincubation at 95°C and 40 cycles at 95°C for 15s for denaturation / 55°C for 30s for annealing / 60°C

for 30s for elongation. Primers are detailed in Appendix I. Beta-actin (*Actb*) was used as a reference gene.

2.8 Statistical analyses

Both data in figures and the text were presented as mean ± standard error of the mean (SEM). To compare the means of groups, one-way analysis of variance (ANOVA) or Welch's t-test (if only two groups) was conducted. For post hoc pairwise comparisons, Tukey's HSD was used. Statistical analyses and generation of figures were done in the R (4.2.1) software environment. For a full list of R packages, please refer to the list of references.

3. Results

I first examined the SSC frequency of intact mouse testes at four stages in postnatal development. I harvested donor testis cells at different ages without any purification and transplanted them individually. Including adults (2-4 months postpartum), I examined pups at three different points in prepuberty: Postnatal day (P)0-2, P6-8, and P16-18. It has been reported that the frequency of SSCs increases from P0-2, reaching the highest level at P6-8 before declining towards adult ages (Shinohara et al., 2001). As shown in Fig. 6A, I found that SSC numbers increased from P0-2 at 6.5 ± 0.7 colonies per 10^5 cells transplanted to 39.0 ± 2.5 colonies at P6-8, followed by a decline to 15.4 ± 1.9 at P16-18 and 2.6 ± 0.2 at adult. This decline is likely caused by an increase in the number of mature germ cells, particularly meiotic and haploid cells with no stem cell activity, which reduces the proportion of SSCs in male germ cells.

On the other hand, the total number of testis cells increased with age, as spermatogenesis was initiated after birth and reached the steady state in adult (Table 3).

Age	Col#/ 10^5 cells	Col#/Donor T	% of Adult	Average T weight	Col#/mg testis	Cell Recovery# /T (x 10^6)
Adult	2.6 ± 0.2	736.5	100%	101.4 mg	7.3 col/mg	27.7
P16-18	15.4 ± 1.9	392.0	53.2%	13.6 mg	28.8 col/mg	2.7
P6-8	39.0 ± 2.5	277.8	37.7%	1.7 mg	168.3 col/mg	0.8
P0-2	6.5 ± 0.7	31.9	4.3%	0.6 mg	49.8 col/mg	0.5

Table 3. Weight, cell recovery, and number of colonies per testis increases with age in mouse. T: testis, Col: colonies. Three biologically independent replicates were performed for each age group. Cell suspensions were prepared by digesting testes with trypsin, in contrast to the remaining experiments of this thesis in which cell dissociation buffer was used.

3.1 Flow cytometric fractionation of testicular cells and identification of the fractions that contain regenerative SSCs.

I used flow cytometry to analyze the expression of cell-surface markers THY1 and ITGA6 throughout postnatal development. I selected these two markers because past studies reported that THY1 is a cell-surface antigen that allows for the best SSC enrichment when used as a single marker (Kubota et al., 2003) while ITGA6 is also an effective SSC marker (Shinohara et al., 2000, 1999). In addition, data of past studies from my lab showed that either loss of THY1 or ITGA6 in adult mouse testes resulted in complete depletion of SSCs; thus, a loss of either protein corresponds to the exit from the stem cell state. I therefore fractionated pup testis cells using THY1 and ITGA6 (Fig. 6B-D). Note that I was able to visualize THY1+ cells in pups with whole-mount immunofluorescence which has been difficult in the past, and as Fig. 6B shows, THY1+ cells were rarely found and were mostly single cells.

Flow cytometric data at four stages of postnatal development are shown in Fig. 6C (right column). Overall, five fractions were identified and were labelled alphabetically from A to E. At P0-2, there are only three fractions, which I labelled A (THY1+ ITGA6+), B (THY1– ITGA6^{hi}), and D (THY1– ITGA6–). The cell fraction that corresponds to C (THY1– ITGA6^{mid}) has not yet developed, in contrast to the profile at P8-9. This three-fraction pattern (Fractions A, B, and D) continued until P8-9, although the immunophenotype of Fraction A shifted (increase in ITGA6 and decrease in THY1), as seen at P6 (Fig. 6). All

five fractions appear at P8-9, including C (THY1– ITGA6^{mid}) and E (THY1+ ITGA6–). This is arguably the most distinct time point in postnatal development because Fraction C emerges. Fraction C and Fraction B appear to overlap, but as described later in Fig. 6D, the majority of cells in Fraction C likely emerge from Fraction A, rather than Fraction B. From P8-9 to P16-18, there is a large increase in the number of cells in Fraction C (14.9% at P8-9 to 65.1% at P16-18), while Fraction B seems to become undetectable by P16 (Fig. 6A). Gradual changes in THY1/ITGA6 expression profiles over time are presented in Fig.13 (Appendix), showing intermediate developmental states at P4, P6, P12, and P14.

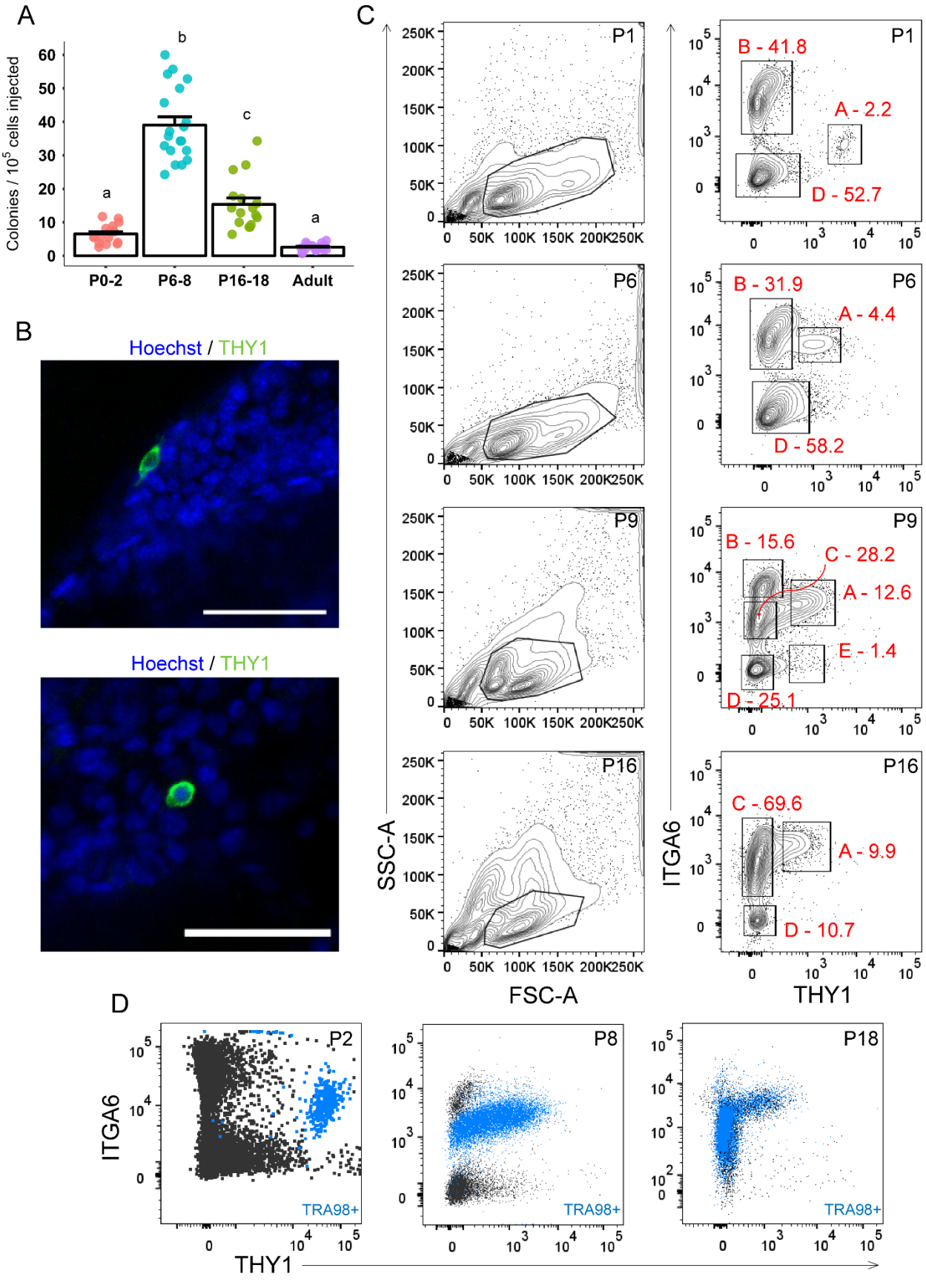
A
Colonies / 10^5 cells injected
60
50
40
30
20
10
0
a
b
c
a
P0-2
P6-8
P16-18
Adult
B
Hoechst / THY1
Hoechst / THY1
C
P1
P6
P9
P16
250K
200K
150K
100K
50K
0
0 50K 100K 150K 200K250K
SSC-A
FSC-A
B - 41.8
A - 2.2
D - 52.7
B - 31.9
A - 4.4
D - 58.2
B - 15.6
C - 28.2
A - 12.6
E - 1.4
D - 25.1
C - 69.6
A - 9.9
D - 10.7
ITGA6
THY1
D
P2
P8
P18
TRA98+
ITGA6
THY1

Figure 6. Mouse testis cells possess distinct levels of regenerative activity throughout developmental stages and show stage specific profiles in flow cytometric analyses.

(A) A single cell suspension of intact mouse testes at each age was assessed for SSC frequency using the transplantation assay. The results are expressed as the number of colonies of donor-derived spermatogenesis per 10^5 cells transplanted. Each dot represents a result from one recipient testis. Three independent biological replicates using testes from different litters were conducted for each age group. Pairwise comparisons were conducted with Tukey's HSD. Alphabet labels ('a', 'b', 'c') indicate statistical significance between two distinct labels ($p < 0.01$ between P0-2 and P16-18; $p < 0.001$ for all other pairs of distinct alphabets).

(B) Whole-mount immunofluorescent staining for THY1 (green) in P9 mouse seminiferous tubules. During this procedure, the seminiferous tubules are placed onto a microscope slide with minimal digestion or disintegration, preserving the overall structure of the tubules. In general, THY1+ cells were sparsely scattered throughout tubules. Some THY1+ cells seemed to clearly lie along the basement membrane, as implied by their morphology (top image). Scale bars, 50 μm.

(C) Multiple cell fractions were identified in mouse testes by flow cytometry based on expression of THY1 and ITGA6. Progression of stage specific profiles is evident during postnatal development. Plots on the left column show profiles of forward scatter (FSC) and side scatter (SSC) of all events. Cells low in side scatter (SSC) were selected, as SSCs are known to localize to this light scatter profile (Shinohara et al., 2000). Plots on the right column show THY1/ITGA6 profiles of the low-side-scatter cell group gated from the left column at each developmental stage. Cells analyzed here were derived from the low-side-scatter cell group and further selected by removing the cells expressing any of the following negative markers: MHC-I (H-2K^b/H-2D^b), CD45, and CD74. Fractions are labelled with black rectangles, and the identification of each fraction found was indicated in red (Fractions A to E) with its population size (% among all the cells analyzed in each profile chart on the right column).

(D) Flow cytometric profiles showing results of intracellular flow cytometry to detect the cells expressing intranuclear germ cell marker TRA98 at three developmental stages. Cells expressing TRA98 are germ cells and colored in blue.

I identified P0-2, P8-9, and P16-18 as three stages in postnatal development with distinct, representative THY/ITGA6 profiles. Although P6 is often considered to be a critical transition period of prepubertal spermatogonia (Bellve et al., 1977; McCarrey, 2017; Yoshinaga et al., 1991), the flow cytometric profile at this age was similar to the profile at P0-2 (Fig. 6C). All other time points postnatally that I assessed had a THY1/ITGA6 profile that was analogous or intermediate to one of these three developmental stages, with a gradual change throughout postnatal development (Fig.

13). Thus, the data obtained demonstrated that distinctive THY1/ITGA6 profiles are established at three developmental stages after birth and shift gradually through postnatal development, leading me to focus my study on these distinct stages.

Flow cytometry and FACS are techniques that segregate cell populations with a high level of resolution, yet have their own technical limitations. For instance, we used MHC-I (H-2K^{b}/H-2D^{b}) as a somatic marker, but consistently observed only a small proportion of MHC-I+ cells, up to ~15% of total cells analyzed. The testis is a complex organ with multiple cell types being the organ constituents, and germ cells are encapsulated in the seminiferous epithelium, which include somatic supporting cells: i.e., Sertoli cells. Thus, the cell fractions shown in Fig. 6C likely include somatic cells. Sertoli cells have been reported to comprise 73% of cells in the seminiferous epithelium at P8 and 29% of cells at P18 (Bellve et al., 1977); it would thus be reasonable to expect more MHC-I+ cells in our testis cell preparation.

To identify germ cells in our flow cytometric profile, I performed intracellular flow cytometry to examine TRA98 expression. The TRA98 antibody reacts with GENA 110 (germ cell-specific nuclear antigen), and its expression is limited to germ cells from the stages of PGCs to spermatids. GENA is not expressed in elongated spermatids or spermatozoa (Tanaka et al., 1998). Fig. 6D shows the expression patterns of TRA98+ cells at each of the three developmental stages.

TRA98 expression is limited to Fraction A at P0-2, with 94.8% of cells in this fraction being TRA98+. At P8-9, Fraction A remains a major germ cell fraction (90.4% of the fraction is TRA98+), and the newly emerged Fraction C also consists mostly of germ cells (73.5%). I suspect the lower proportion of TRA98+ cells in Fraction C is due to overlap with Fraction B (TRA98–). In terms of the entire germ cell population, Fraction A comprises 48.3% of male germ cells at P8-9 while Fraction C comprises 50.7%, indicating that the two fractions are similar in germ cell number at this stage.

At P16-18, Fraction A retains a similar proportion of TRA98+ cells (91.2% of fraction is TRA98+) while Fraction C has an increased proportion of TRA98+ cells (89.6%) compared to P8-9. Interestingly, Fraction C is now a dominant germ cell fraction, comprising 83.3% of the entire germ cells at P16-18, in comparison to Fraction A being

only 12.1%, suggesting an ongoing commitment process of germ cell development after birth. In summary, Fractions A and C are the major germ cell fractions at all three time points. Furthermore, our data agrees well with previous studies (Bellve et al., 1977): Fractions A and C combine to 26.4% of the testicular single cell suspension at P8-9, which is comparable to 27% germ cells at P8 as reported by Bellve et al., 1977. Likewise, 74.4% of the parent population at P16-18 in my study is comparable to 71% germ cells at P18 by Bellve et al., 1977.

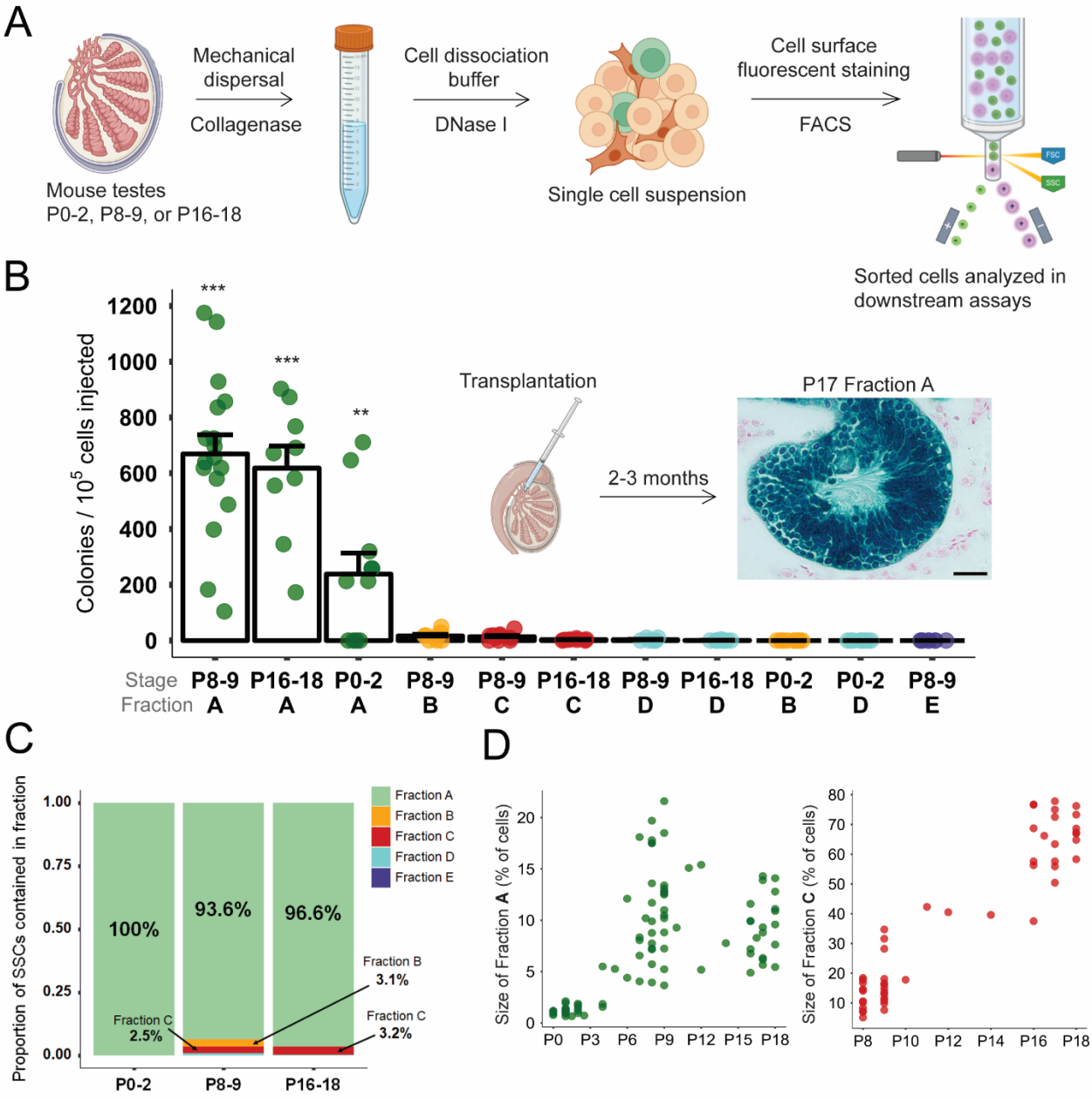

Figure 7. Fraction A contains nearly all regenerative cells regardless of age.

(A) Schematic representation of the procedure from the preparation of a single cell suspension of testes to fractionation using FACS.

(B) Colony numbers of donor-derived spermatogenesis determined by the transplantation assay. Fractions were sorted using FACS and transplanted into recipient testes to examine regenerative activity. Each point represents data from one recipient testes. Fractions on the X-axis are ordered by SSC enrichment. For statistics, fractions were compared within developmental stages by pairwise comparisons with Tukey's HSD (* $p < 0.05$; ** $p < 0.01$; *** $p < 0.001$). The inset shows a histological section of recipient testes after transplantation of cells from Fraction A in P17 ROSA pups. Testes were

stained with X-gal, labelling donor cells derived from ROSA26 mice with a blue color. Note the tails of spermatozoa in the lumen of the seminiferous tubule, demonstrating the complete regeneration of spermatogenesis. Scale bar, 50 μm.

(C) The proportion of SSCs contained in fractions at each developmental stage. Calculated as the product of the SSC enrichment in each fraction (number of colonies per 10^5 cells transplanted) and the population size of each fraction at a given stage (% of cells in each fraction according to the THY1/ITGA6 flow profile).

(D) Proportions of Fraction A and Fraction C in germ cell population throughout postnatal development. “Size” here refers to the % of cells that each fraction contains in the total events captured in the THY1/ITGA6 flow profile as in Fig. 6C. Note that X-axis begins at different ages (P0 for Frac. A, P8 for Frac C). Mean size of Fraction A at P0-2: 1.22% ± 0.08%, P8-9: 11.51% ± 0.91%, P16-18: 9.27% ± 0.64%.

Data shown in Fig. 6 demonstrate that germ cell populations shift their flow cytometric profiles over time during their development. Then, it is logical to ask in which fraction regenerative SSCs are located and if these stem cells stay in the same fraction throughout development or if their profiles shift over time. To address these questions, I determined the frequency of SSCs using FACS to sort individual fractions (Fig. 7A). Cells were transplanted into recipient mouse testes to functionally quantify regenerative cells in each fraction. The transplantation assay detects the ability of cells to self-renew and reconstitute spermatogenesis and is therefore the unequivocal assay to determine SSC activity.

I found that at all three developmental stages, Fraction A contains the vast majority of SSCs, and the frequency of SSCs is negligible in other Fractions (Fig. 7B). Fraction A at P8-9 and P16-18 retained a similar amount of SSC enrichment (669.2 ± 69.0 and 618.1 ± 79.4 colonies per 10^5 cells transplanted, respectively), while at P0-2 there was a lower level of enrichment (238.3 ± 75.4). Yet, Fraction A was the only cell group with SSC identities at P0-2. Importantly, I found that all fractions other than Fraction A, including Fraction C, contain only negligible levels of SSCs or none at all (Fig. 7C). I therefore consider Fraction A, which has the immunophenotype of THY1+ ITGA6+, to be *the* stem cell fraction throughout postnatal development. These results support the notion that loss in expression of THY1 or ITGA6 corresponds to exit from the SSC state in mice.

It is interesting that SSC frequency is similar in Fraction A at P8-9 and P16-18, but significantly lower at P0-2 (Fig. 7B). This observation suggests a potential difference in regenerative activity between prospermatogonia, which are present in P0-2, and spermatogonia. While there are many differences between prospermatogonia and spermatogonia, such as their location in the seminiferous tubules, stage in the cell cycle, the amount of signaling factors like retinoic acid (Busada et al., 2014), and gene expression profile (Tan et al., 2020), it is not known what exactly causes the difference in regenerative activity. For example, prospermatogonia are still detached from the basement membrane, which could reflect a lower ability in homing to the basement membrane following transplantation, resulting in lower regenerative activity. Furthermore, there are epigenetic differences in postnatal prospermatogonia when compared to spermatogonia, which may contribute to differences in regenerative activity, such as high expression of the DNA methyltransferase enzyme DNMT3A2 (Shirakawa et al., 2013) and high levels of CH (H = A, C, or T) methylation (Kubo et al., 2015). DNMT3A2 expression is elevated in committed progenitors (P7.5 PLZF– KIT+ spermatogonia), which have reduced regenerative activity (Shirakawa et al., 2013). Furthermore, DNMT3A (DNMT3A2 is an isoform of DNMT3A) catalyzes CH methylation, although the functional role of CH methylation is unclear (Guo et al., 2014).

Alternatively, P0-2 Fraction A is comprised of two populations, one that will differentiate into the first wave (eventually forming sperm) and another that will form the SSC pool (de Rooij, 1998). I hypothesize that at P8-9, germ cells are separated into Fraction A (SSC pool) and Fraction C (commitment to the first wave). In this case, Fraction A at P8-9 would naturally have higher SSC enrichment than at P0-2, because at P0-2 there still are first wave precursors (committed, SSC-depleted) in Fraction A.

Fraction C is a germ cell fraction, yet only has a small amount of SSC activity (13.7 ± 4.2 at P8-9 and 2.9 ± 0.9 at P16-18). The size of Fraction C continually increases throughout postnatal development (50.7% of total germ cell population at P8-9 to 83.3% at P16-18) after it appears at P8-9. Fraction A, on the other hand, does not increase in size past P8-9, and instead continues to slowly shrink (48.3% of total germ cell population at P8-9 to 12.1% at P16-18). These observations support the idea that

Fraction C is comprised of differentiating cells which form the first wave and have progressed far enough in commitment such that all regenerative activity is lost (Fig. 7B). Note that the number of KIT-expressing cells in Fraction C rapidly increases from 29.2% ± 1.8% at P8-9 to 61.4% ± 3.3% at P16-18 (Fig. 14, Appendix). The number of cells in Fraction A seems to be maintained (Fig. 7D) rather than constantly expanding like Fraction C.

3.2 Identifying the fractions that contain cluster-forming cells at each stage.

Considering that Fraction A contains all regenerative cells in vivo, one might expect its stem cell activity to be retained in vitro. In order to regenerate spermatogenesis after transplantation, cells must proliferate and differentiate. Thus, I hypothesized that the cells in a specific fraction which is enriched for regenerative cells can proliferate and have the capacity to generate spermatogonial aggregation, which we call “clusters”, in vitro. Importantly, the numbers of clusters in vitro is correlated to the number of colonies formed in vivo when those cells are transplanted (Yeh et al., 2007); i.e., cluster numbers correspond to the quantity of regenerative stem cells.

To test this hypothesis, I conducted short-term cluster-forming assays as in Yeh et al., 2007. Fractionated cells were cultured for 6-7 days and clusters were visually counted at the end of the culture period after fixing the culture wells with glutaraldehyde.

The results showed that cluster-forming activity was contained predominantly in Fraction A at all three developmental stages (Fig. 8A). Only negligible activity was noted in Fraction C at P8-9 (3.1 ± 1.0 clusters / 10^5 cells seeded). In this aspect, the levels and distribution of cluster-forming activity among different ages and fractions resembled those of regenerative activity in vivo (Fig. 7B). One difference is that cluster-forming activity in Fraction A at P16-18 (816.7 ± 174.1) was more than double of that at P8-9 (334.5 ± 68.1), whereas they were quite similar in regenerative activity (Fig. 7B).

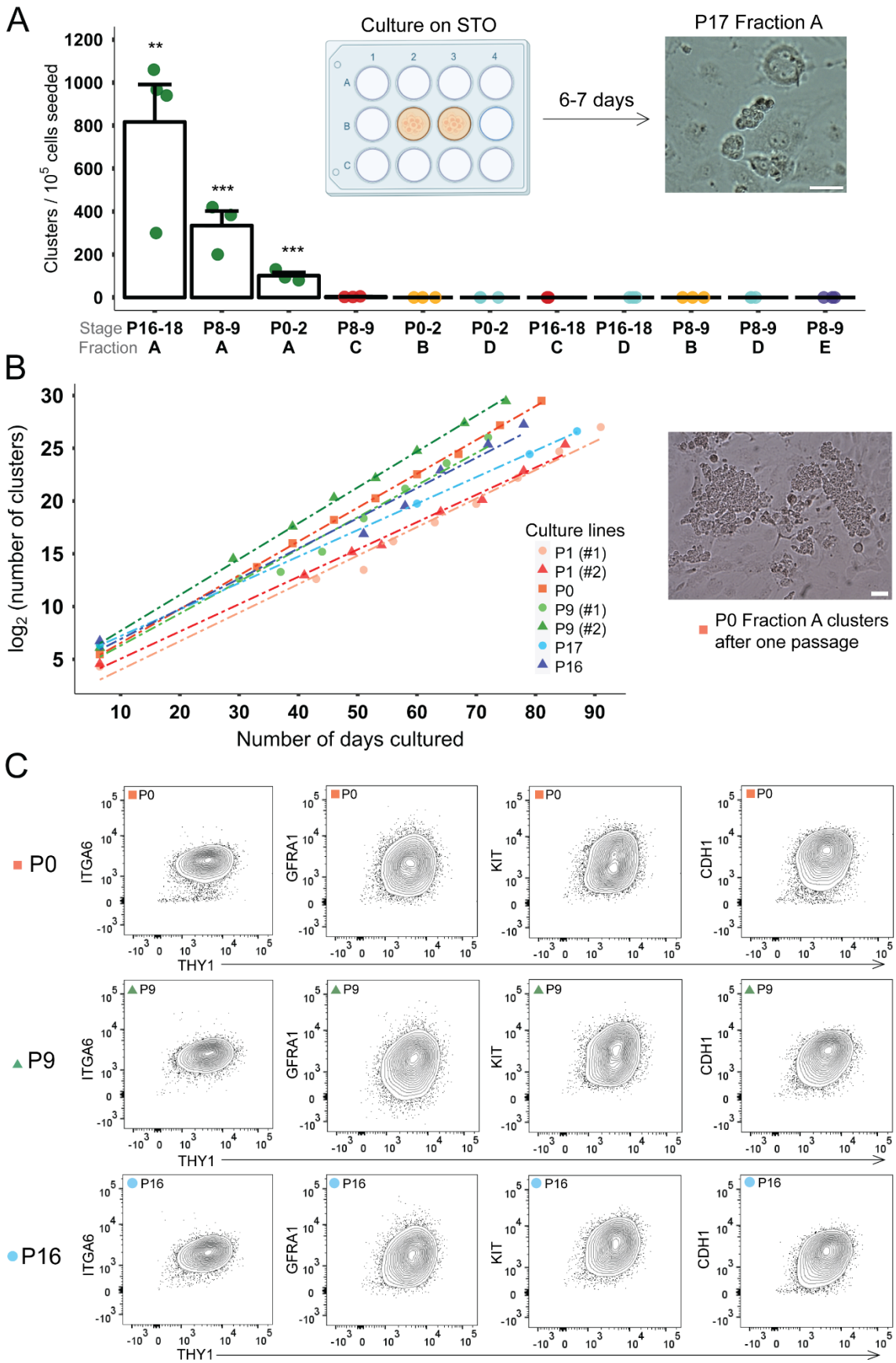
A
Culture on STO
P17 Fraction A
6-7 days
Clusters / 10^5 cells seeded
1200
1000
800
600
400
200
0
**
***
***
Stage P16-18 P8-9 P0-2 P8-9 P0-2 P0-2 P16-18 P16-18 P8-9 P8-9 P8-9
Fraction A A A C B D C D B D E
B
log2 (number of clusters)
30
25
20
15
10
5
10 20 30 40 50 60 70 80 90
Number of days cultured
Culture lines
P1 (#1)
P1 (#2)
P0
P9 (#1)
P9 (#2)
P17
P16
P0 Fraction A clusters after one passage
C
P0
P9
P16
ITGA6
GFRA1
KIT
CDH1
THY1

Figure 8. Fraction A contains all cluster-forming activity in vitro regardless of age and can be used to generate long-term culture lines.

(A) Cluster-forming activity of all fractions evaluated with the short-term in vitro assay. Cells were sorted with FACS and cultured for 6-7 days on a 48-well plate without subculturing. Fractions on the X-axis are ordered by the level of cluster-forming activity. Up to four independent biological replicates using testes from different litters of mice were conducted for each age group. For statistics, fractions were compared within developmental stages, pairwise comparisons conducted with Tukey's HSD (* $p < 0.05$; ** $p < 0.01$; *** $p < 0.001$). Scale bar, 50 μm.

(B) Long-term culture and expansion of seven cluster lines derived from ROSA26 mice (each line denoted by a different color). Fraction A cells of ROSA26 pups at three different developmental stages were cultured for up to 91 days. The number of clusters after the first week was derived from Fig. 8A. Thereafter, the numbers were counted visually at each passage. The P17 culture line was frozen after eight passages and thawed to resume culture; two data points are from the period after thawing. The inset shows a typical morphology of a cluster. Scale bar, 50 μm.

(C) Representative flow cytometric profiles at each developmental stage. Culture lines were analyzed after 10 passages. Five surface markers were examined: THY1, ITGA6, GFRA1, KIT, and CDH1.

After finding that Fraction A contains all cluster-forming activity, I established long-term culture lines from Fraction A cells; I trypsinized clusters after 9-14 days of initial culture and reseeded a portion of the cells harvested onto a newly prepared feeder layer to continue cluster culture. Characteristics of all culture lines generated are listed in Table 4.

Pup Age	Length of culture period	Doubling time (days)	Total fold expansion
P1	91 days (10 passages)	3.70	6.82×10^6
P1	85 days (9 passages)	3.86	1.81×10^6
P0	81 days (10 passages)	3.12	1.70×10^7
P9	72 days (9 passages)	3.29	8.41×10^5
P9	75 days (9 passages)	2.94	1.08×10^7
P17	87 days (11 passages)	3.98	1.28×10^6
P16	78 days (9 passages)	3.49	1.51×10^6

Table 4. List of ROSA long-term culture lines generated by sorting Fraction A. "Doubling time" is the number of days calculated for the number of clusters to double. "Total fold expansion" refers to growth in the number of clusters, compared to the number of clusters at P0 (after 6-7 days in vitro). These were derived from the data shown in Fig. 8A.

I generated seven culture lines total (Table 4) and counted the number of clusters at the time of passaging to calculate the rate of expansion (Fig. 8B). The rate of expansion is represented by the "doubling time" in Table 4, which is the number of days required for the number of clusters to double. P0-2 culture lines averaged a doubling time of 3.6 days, P8-9 culture lines averaged 3.1 days, and P16-18 culture lines averaged 3.7 days. I initially suspected that P0-2 Fraction A cells would have a rate of proliferation slower than P8-9 or P16-18 because they had lower short-term cluster-forming activity. However, I found their proliferative activity long-term comparable to P8-9 or P16-18 culture lines. Interestingly, long-term proliferative activity (2-3 months) was different from short-term cluster-forming activity (6-7 days) examined with the CFA.

Next, I analyzed the flow cytometric profile of all cluster lines for the expression of five cell-surface markers: THY1, ITGA6, GFRA1, KIT, and CDH1 (Fig. 8C). All five surface markers (THY1, ITGA6, GFRA1, KIT, CDH1) were clearly expressed in all cultures analyzed. When two-parameter profiling was performed, we found only one "fraction" on the profile chart; cells exhibited a profile with one single oval shape (Fig. 8C). In contrast, testis cells formed multiple fractions (Fig. 6C). This implies that cluster cells in vitro are more uniform in comparison to the cell population prepared from testis, which may contain germ cells at different levels of commitment and somatic cells. Furthermore, it is notable that we do not clearly see developmental stage-dependent marker expression patterns (P0-2, P8-9, P16-18).

Importantly, KIT expression was similar across all cultures, and P0-2 cultures expressed KIT at levels comparable to P8-9 and P16-18 clusters after long-term culture (Fig. 8C). Interestingly, as described later in Fig. 11A, P0 Fraction A in vivo has virtually no KIT expression, consistent with past studies (Niedenberger et al., 2015; Ohbo et al., 2003; Yoshinaga et al., 1991). It is likely that P0-2 cells mature during long-term culture or adopt to an in vitro environment, leading to the emergence of KIT+ cells at a similar

level as observed with P8-9 and P16-18 cells. This maturation may also be reflected by the fact that P0-2 clusters show proliferative activity comparable to P8-9 and P16-18 clusters (Fig. 8B, Table 4). KIT expression in SSC culture has been reported in several studies, but interestingly, KIT expression seems to be nonessential for proliferative activity in vitro (Kanatsu-Shinohara et al., 2003; Morimoto et al., 2009)

3.3 Gene expression analyses of germ cell fractions of mouse testes

To characterize the in vivo germ cell fractions (Fractions A and C, Fig. 6C) at the molecular level, I analyzed the transcripts of spermatogonial marker genes using quantitative real-time PCR. I examined a panel of 12 genes, five of which are considered to be SSC/self-renewal markers (*Gfra1*, *Id4*, *Etv5*, *Nanos2*, *Zbtb16*), four progenitor markers (*Nanos3*, *Neurog3*, *Sohlh1*, *Sohlh2*), and two differentiation markers (*Kit*, *Stra8*). I also included a Sertoli cell marker, *Wt1* (Chen et al., 2022), to this panel of spermatogonial genes. Fig. 9A displays a summary of the results in a heatmap. Rows were grouped using the R package pheatmap, in order to identify sets of genes that had similar expression patterns (Raivo Kolde, 2019). Complete-linkage clustering was performed based on Euclidean distance. WT1 was excluded from the hierarchical clustering algorithm because it is uniquely a Sertoli cell marker.

Genes can be largely divided into three groups based on hierarchical clustering: group 1 (*Gfra1*, *Id4*, *Etv5*, and *Nanos2*), group 2 (*Zbtb16*, *Nanos3*, *Neurog3*, *Sohlh1*, *Sohlh2*), and group 3 (*Kit*, *Stra8*). This grouping is mostly similar to the previous understanding of these genes, assuming that group 1 is the SSC/self-renewal markers, group 2 is the progenitor markers, and group 3 is the differentiation markers. One exception might be *Zbtb16*, which is believed to be essential in spermatogonial self-renewal (Costoya et al., 2004).

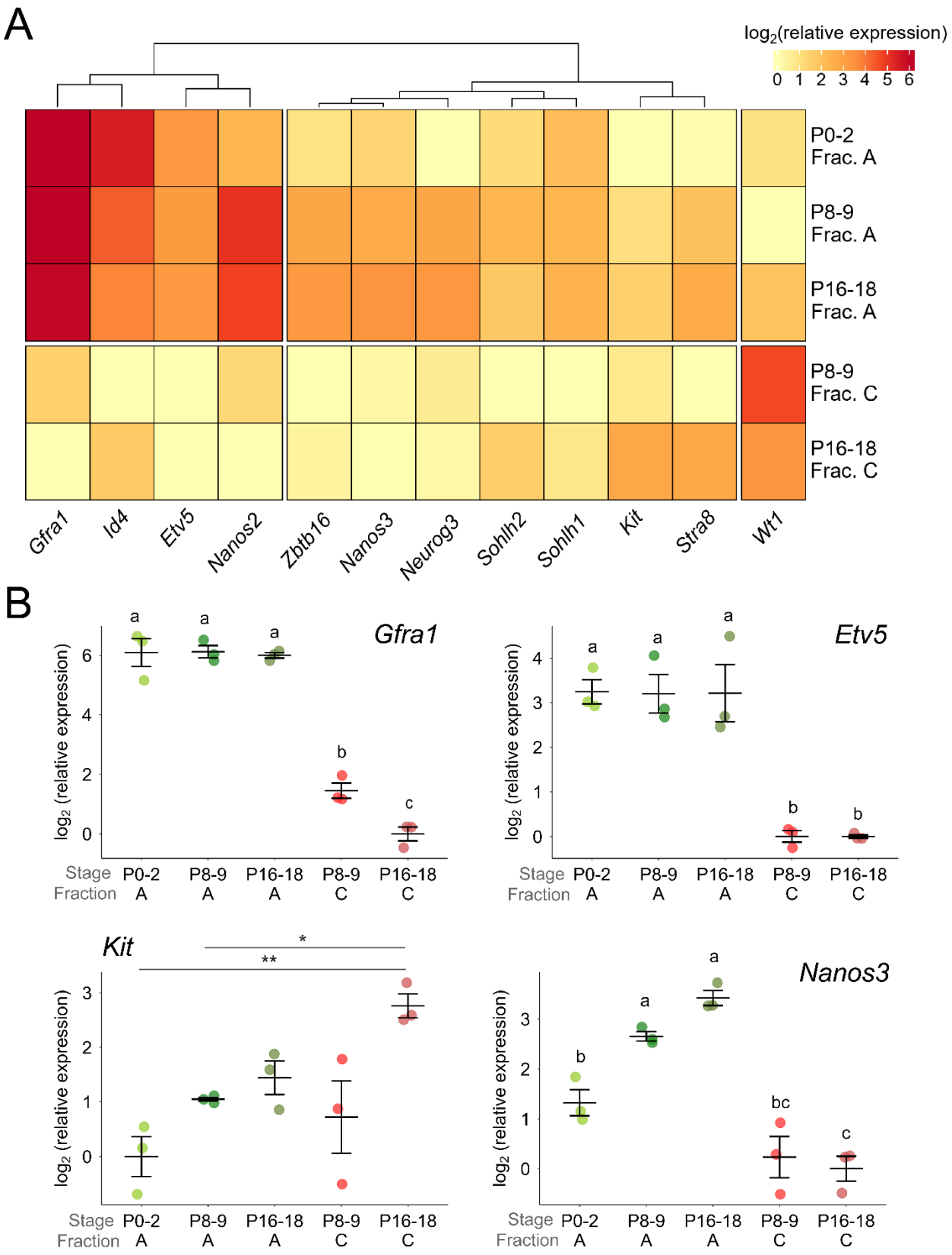
A
log2(relative expression)
0 1 2 3 4 5 6
P0-2 Frac. A
P8-9 Frac. A
P16-18 Frac. A
P8-9 Frac. C
P16-18 Frac. C
Gfra1
Id4
Etv5
Nanos2
Zbtb16
Nanos3
Neurog3
Sohlh2
Sohlh1
Kit
Stra8
Wt1
B
Gfra1
Etv5
Kit
Nanos3
log2 (relative expression)
Stage P0-2 P8-9 P16-18 P8-9 P16-18
Fraction A A A C C
a a a b c
a a a b b
* **
b a a bc c

Figure 9. Fraction A cells express transcripts of SSC, progenitor, and differentiation marker genes.

(A) Expression of key genes in Fractions A and C at the three developmental stages. Quantitative real-time PCR was conducted to compare the relative expression of 12 genes in germ cell fractions from three developmental stages. For each fraction, three independent biological replicates were collected.

(B) Relative expression of four selected genes (*Gfra1*, *Etv5*, *Nanos3*, *Kit*) in Fractions A and C at the three developmental stages, measured with RT-qPCR. *Actb* was used as a reference gene for normalization. Three independent biological replicates were collected for each fraction and age. Mean expression was compared with a one-way ANOVA, and pairwise comparisons were conducted with Tukey's HSD (* $p < 0.05$; ** $p < 0.01$; *** $p < 0.001$). Data for the remaining eight genes are shown in Figure 16, Appendix 6.5. Alphabet labels ('a', 'b', 'c') indicate statistical significance between two distinct labels. As for 'ab', it is significantly different from 'c' but not from 'a' or 'b'.

Gfra1, *Id4*, *Etv5*, and *Nanos2* were identified as one group of genes with similar expression patterns. Generally, these four genes were highly expressed in Fraction A while at reduced levels in Fraction C across the three developmental stages. *Gfra1* and *Etv5* were uniformly expressed in Fraction A across the three time points, but *Id4* showed the highest expression at P0-2, and *Nanos2* showed the highest expression at P8-9.

Zbtb16, *Nanos3*, and *Neurog3* were similar in their expression patterns and were most highly expressed at P8-9 and P16-18 in Fraction A. *Sohlh1* and *Sohlh2* showed a similar trend of expression patterns as *Zbtb16*, *Nanos3*, and *Neurog3*. *Kit* and *Stra8* were similar to each other, and differ from the aforementioned five genes in that they were highly expressed in P16-18 Fraction C. Finally, *Wt1* was most highly expressed in P8-9 Fraction C, followed by P16-18 Fraction C. This is consistent with my intracellular flow cytometry results (Fig. 6D) in which P8-9 Fraction C had more somatic cell contamination (26.5% TRA98–) than P16-18 Fraction C (10.4% TRA98–).

In summary, Fraction A contains not only SSCs, but also progenitors and differentiating cells, as characterized by expression patterns of key marker genes. For example, *Kit* was expressed in P8-9 and P16-18 Fraction A. This observation leads to the notion that Fraction A could be further separated into populations that are more SSC-like (e.g., KIT–) and those that are more progenitor-like (KIT+). Comparing Fraction A across the

developmental stages, I found that gene expression patterns at P8-9 and P16-18 were similar, but those at P0-2 were quite distinct. First, expression of *Id4* was higher and *Nanos2* was lower at P0-2, which could be related to the lower amount of regenerative activity (669.2 ± 69.0 colonies per 10^5 cells transplanted at P8-9 and 618.1 ± 79.4 at P16-18, versus 238.3 ± 75.4 at P0-2, Fig. 7B). Second, expression of progenitor genes (*Nanos3*, *Neurog3*, *Sohlh1*, *Sohlh2*) and differentiation genes (*Stra8*, *Kit*) were lower at P0-2. This supports the notion that P0-2 Fraction A contains the cells that are less committed to differentiation in general, compared to P8-9 or P16-18. Further characterization of a "SSC-like" subpopulation and a more "putative first wave" subpopulation at P0-2 may require in-depth analyses, such as those based on scRNA-seq. In this regard, a recent scRNA-seq study (Tan et al., 2020) suggests two subpopulations at P2 that can be divided based on the expression of cell-cycle genes, including *Ccnd2* and *Ttc28*.

My RT-qPCR analysis demonstrates that Fraction A at P8-9 and P16-18 contains the cells that express transcripts of SSC/self-renewal (*Gfra1*, *Id4*, *Etv5*, *Nanos2*, *Zbtb16*), progenitor (*Nanos3*, *Neurog3*, *Sohlh1*, *Sohlh2*), and/or differentiation genes (*Stra8*, *Kit*), and thus, could be further fractionated into subpopulations that are more and others that are less committed to differentiation. This conclusion led me to attempt further subfractionation of Fraction A using additional surface markers.

3.4 Further subfractionation of Fraction A derived from testes

To subdivide Fraction A, I selected GFRA1 and KIT as the fractionation parameters for two reasons. One is that these are the markers widely believed to be associated with undifferentiated and differentiating spermatogonia, respectively. The other is that while GFRA1 expression is predominantly seen in Fraction A, KIT expression tends to be localized in Fraction C but also observed in Fraction A at an appreciable level (Fig. 10). Indeed, GFRA1 and KIT appeared to be effective markers to subdivide Fraction A in more focused flow cytometric analyses (Fig. 11A). At P0-2, Fraction A was separable into two fractions: GFRA1+ and GFRA1–. As for KIT expression, the presence of KIT+ cells was negligible (Fig. 11A). This corresponds to the reports that KIT expression is

generally absent at the protein level in prospermatogonia and begins around P3.5-4 (Niedenberger et al., 2015; Ohbo et al., 2003; Yoshinaga et al., 1991). Thus, these observations give rationale to subfractionate P0-2 Fraction A only into GFRA1+ and GFRA1– cells.

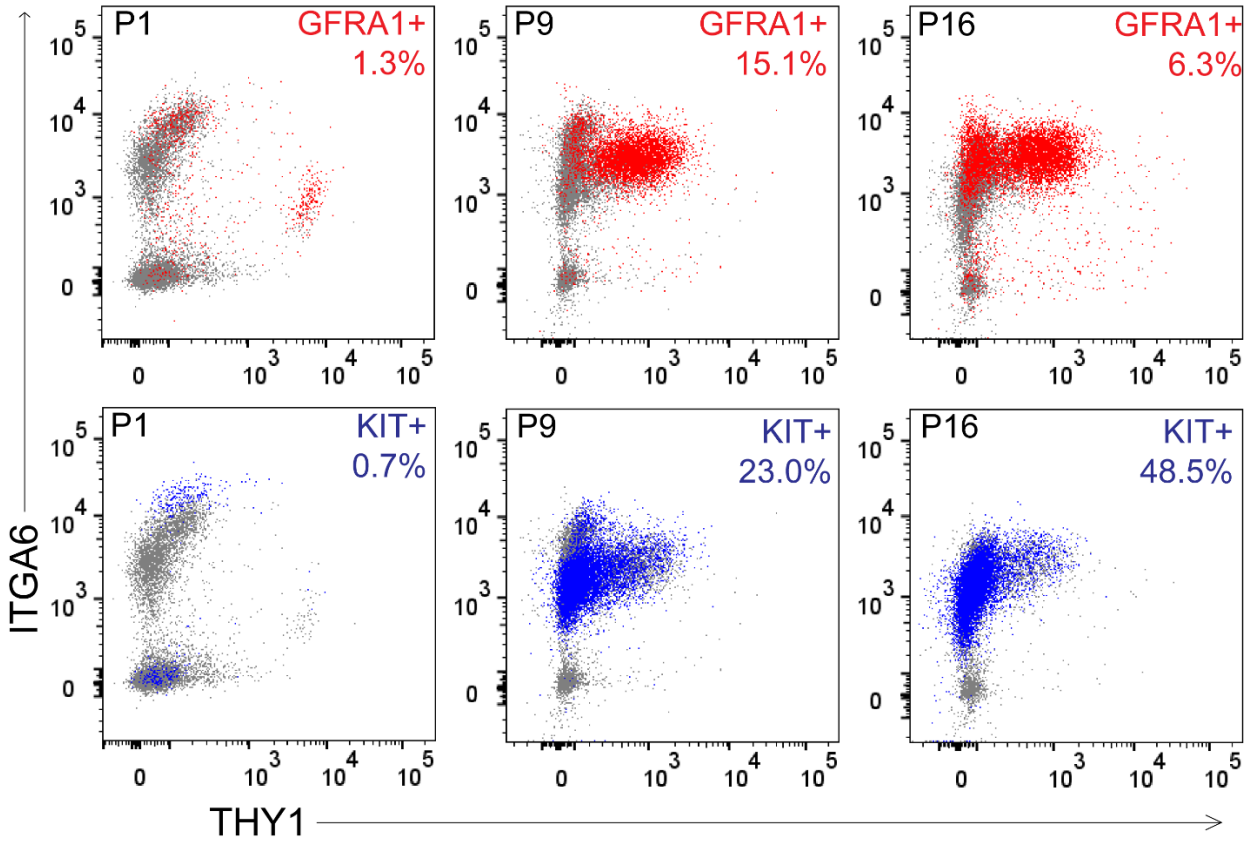

Figure 10. Backgating of GFRA1+ and KIT+ cells onto THY1/ITGA6 profiles at the three developmental stages. Percentage of GFRA1+ and KIT+ cells are indicated in the top right corner of each profile. GFRA1+ and KIT+ cells are marked as red and blue, respectively.

At P8-9 and P16-18, Fraction A was separable into four fractions: GFRA1+ KIT–, GFRA1+ KIT+, GFRA1– KIT–, and GFRA1– KIT+. To my knowledge, this is the first time that mouse pups were fractionated in FACS using both GFRA1 and KIT. It is interesting to note that we detected GFRA1+ KIT+ cells. Although this indicates a simultaneous expression of two proteins that usually depict opposite directions of cell fate status, there are past studies that detected GFRA1+KIT+ spermatogonia (Hofmann et al.,

2005; Nakagawa et al., 2010; Niedenberger et al., 2015). I therefore included these cells for further analyses.

After sorting based on GFRA1 and KIT expression, I examined each subfraction for both regenerative capacity and cluster-forming activity, using spermatogonial transplantation in vivo and the CFA assay in vitro, respectively. Upon transplantation, GFRA1+ cells at P0-2 produced 282.8 ± 128.4 colonies per 10^5 cells transplanted, while GFRA1– cells at P0-2 produced none (Fig. 11B). At P8-9, regeneration of donor-derived spermatogenesis was observed from all subfractions. Among them, GFRA1+ KIT– cells showed the highest level of SSC activity (618.5 ± 94.3 colonies per 10^5 cells transplanted) and GFRA1– KIT+ cells had the lowest activity (122.3 ± 65.7). This lowest level of SSC activity is, however, still higher than that of bulk, unfractionated testis cells. For example, the cells derived from intact testes at P6-8 with no manipulations generate 39.0 ± 2.5 colonies per 10^5 cells transplanted, indicating that GFRA– KIT+ cells in Fraction A at P8-9 are roughly three-fold enriched in SSCs. Finally, at P16-18, GFRA1+ KIT– and GFRA+ KIT+ fractions had similar levels of regeneration capacity (729.3 ± 84.8 and 744.2 ± 104.6 respectively). GFRA1– KIT+ cells once again had the lowest level of activity (67.2 ± 39.6). GFRA1– KIT– cells maintained a similar level of SSC capacity from P8-9 to P16-18 (391.6 ± 62.6 at P8-9 to 384.5 ± 83.4 at P16-18).

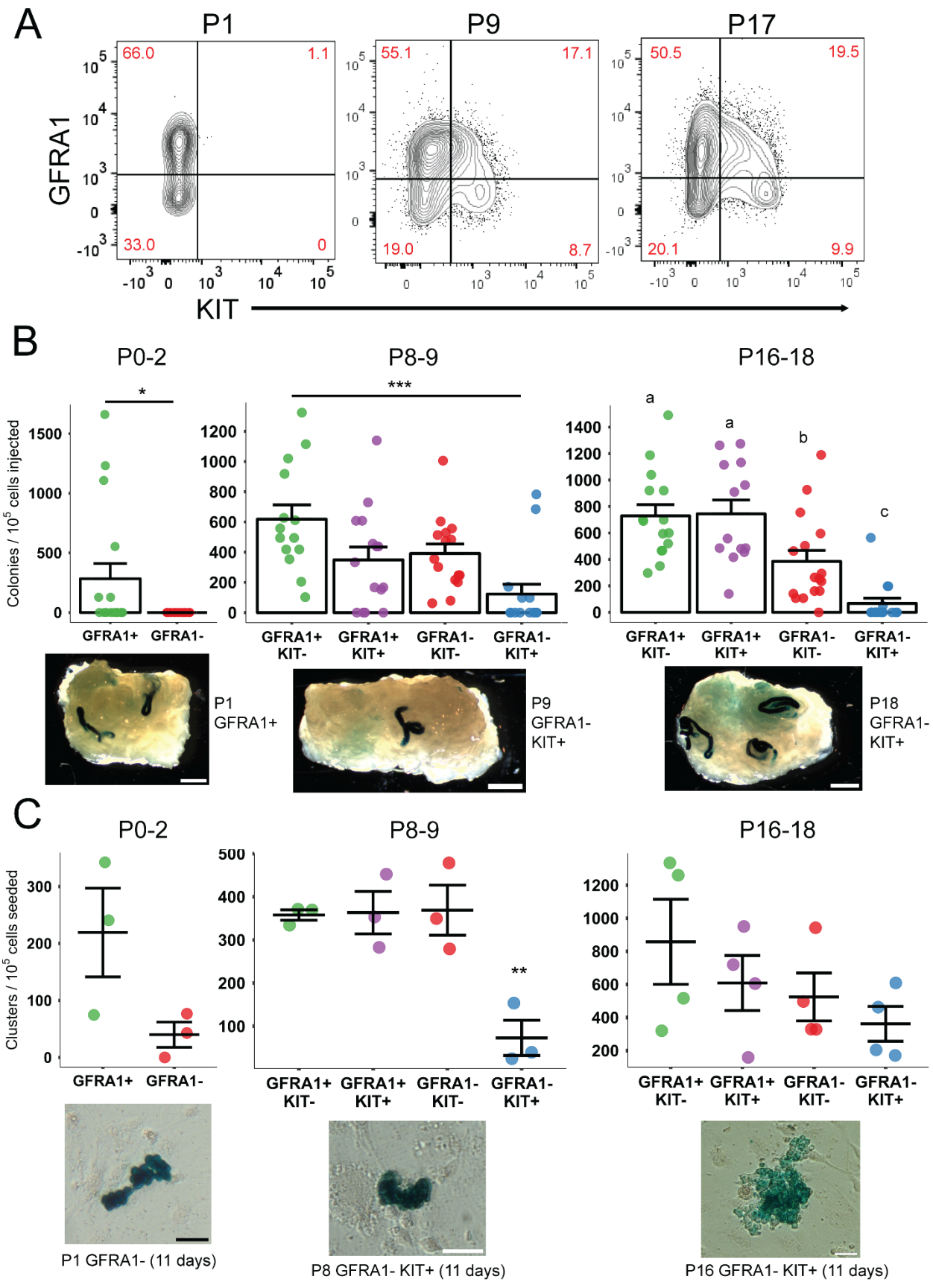
A
P1
P9
P17
66.0
1.1
33.0
0
55.1
17.1
19.0
8.7
50.5
19.5
20.1
9.9
GFRA1
KIT
B
P0-2
P8-9
P16-18
Colonies / 10^5 cells injected
GFRA1+
GFRA1-
GFRA1+ KIT-
GFRA1+ KIT+
GFRA1- KIT-
GFRA1- KIT+
P1 GFRA1+
P9 GFRA1- KIT+
P18 GFRA1- KIT+
C
Clusters / 10^5 cells seeded
P1 GFRA1- (11 days)
P8 GFRA1- KIT+ (11 days)
P16 GFRA1- KIT+ (11 days)

Figure 11. GFRA1 and KIT can further subdivide Fraction and almost all GFRA1 and KIT subfractions retain SSC activity.

(A) GFRA1 and KIT expression of Fraction A at the three developmental stages. Shown are flow cytometric plots depicting GFRA1 and KIT expression patterns of Fraction A at P1, P9, and P17. GFRA1 and KIT subfraction gates were guided by GFRA1 and KIT FMO (Fluorescence Minus One) controls. Size (%) of fractions or quadrants are noted in red.
(B) SSC activity of GFRA1/KIT subfractions as measured by spermatogonial transplantation. Each point represents data from one recipient testes. Three independent biological replicates using testes from different litters were conducted for each developmental stage. Pairwise comparisons conducted with Tukey's HSD (* $p < 0.05$; ** $p < 0.01$; *** $p < 0.001$). Alphabet labels ('a', 'b', 'c') indicate statistical significance two distinct labels ($p < 0.05$ between 'a' and 'b', 'b' and 'c', $p < 0.001$ between 'a' and 'c'). Scale bars, 1 mm.
(C) In vitro cluster forming activity of GFRA1/KIT subfractions. Sorted cells were cultured for 9-11 days on a 48-well plate without subculturing. For each developmental stage, 3-4 independent biological replicates using testes from different litters were conducted. Pairwise comparisons conducted with Tukey's HSD (* $p < 0.05$; ** $p < 0.01$; *** $p < 0.001$). Scale bars, 50 μm.

To summarize, there is a clear trend that GFRA1+ subfractions exhibit more regenerative activity than GFRA– subfractions. In addition, KIT– subfractions show more regenerative activity than KIT+ subfractions. One exception to this trend is that GFRA1+ KIT+ cells had more regenerative activity than GFRA1+ KIT– cells at P16-18 (744.2 ± 104.6 and 729.3 ± 84.8 colonies per 10^5 cells transplanted respectively). Importantly, all subfractions except for P0-2 GFRA1– retained regenerative activity, indicating that even GFRA1– KIT+ cells have not entirely committed to differentiation and lost SSC activity. For example, GFRA1– KIT+ cells at P8-9 regenerated 122.3 ± 65.7 colonies per 10^5 cells transplanted. This is a surprisingly high level, since it leads to an estimate of one SSC in 98 sorted cells, assuming a 12% homing rate after transplantation (Nagano, 2003). The identity of GFRA1– KIT– cells is unclear. Since this cell fraction clearly showed SSC activity higher than GFRA1– KIT+ cells, this result cannot be explained simply by contamination of other fractions. In this regard, Garbuzov et al. reported that GFRA1– cells have SSC capacity and the number of GFRA1– SSCs is similar to the number of GFRA1+ SSCs in adult mice (Garbuzov et al., 2018). More detailed analysis of this cell fraction is necessary in the future.

Next, I determined the cluster-forming activity of each subfraction of Fraction A at three developmental stages (Fig. 11C) and tested the hypothesis that the regeneration potential of subfractions as revealed above (Fig. 11B) reflects the in vitro SSC capacity. For these assays, I extended the assay length from 6-7 days to 9-11 days, with two exchanges of culture medium instead one and with no passaging. I reasoned that this strategy allows smaller clusters to expand further, such that cluster counting would not cause underestimation. As shown in Fig. 11C, the results obtained generally supported the hypothesis. For example, cluster-forming activity at P0-2 mirrored regenerative activity in vivo, with GFRA1+ cells (219.2 ± 77.9 clusters per 10^5 cells seeded) having more activity than GFRA1– cells (40.0 ± 22.2). At P8-9, GFRA1– KIT+ cells (72.8 ± 41.0) had significantly less cluster-forming activity, while all other fractions were similar in activity. Finally, at P16-18, I found that GFRA1– KIT+ cells once again had the lowest cluster-forming activity of all fractions, albeit still high in absolute terms (336.3 ± 86.7).

Taken together, the results demonstrated that nearly all GFRA1/KIT subfractions in Fraction A retain SSC activity at the three developmental stages in vivo and in vitro. Although there are variations in the degree of SSC capacity detected in vivo and in vitro, the SSC status is maintained as long as the cells express both THY1 and ITGA6. In other words, although GFRA1 and KIT are generally accepted as positive and negative markers of SSCs, respectively, these two antigens are incapable of further enriching THY1+ ITGA6+ cells for SSCs. As such, even GFRA1– KIT+ cells are not truly SSC-depleted as long as they express THY1 and ITGA6.

4. Discussion

In this study, I used FACS to extensively fractionate spermatogonia with an 8-color panel (Table 2). Doing so, I described distinct flow cytometric profiles during postnatal mouse development (Fig. 6C). I found that THY1/ITGA6 profiles effectively capture the postnatal development of the testis (Appendix, Fig. 13) and identified P8-9 as a crucial stage when Fraction C, the THY1-negative germ cell fraction, emerges for the first time

after birth. Before conducting flow cytometric analyses, I expected P6-7 to be the crucial developmental stage, as this is widely regarded as an important stage in prepubertal development when spermatogonia have emerged from prospermatogonia (McCarrey, 2017). Instead, Fraction C first appeared at P8-9, which coincides with the appearance of preleptotene spermatocytes (Bellve et al., 1977; Geyer, 2017).

Next, I identified Fraction A as the SSC-enriched fraction throughout postnatal development in vivo and in vitro, and this is the highest level of regenerative activity reported in pups (Table 5). This was achieved from intact testes without any manipulation (e.g. transgenesis), which is promising for clinical translation to hSSC isolation. Some past studies with notable levels of enrichment are listed in Table 6. The technique I established allows for a far higher level of SSC enrichment in THY1+ ITGA6+ CD45– CD74– MHC-I– cells (Fraction A) with a wider range of donor mouse ages (P0 to P18).

Age & Fraction	**Colonies per 10^5 transplanted**	**Fold increase**	**SSC frequency (Fraction A)**	**SSC frequency (unsorted)**
P0-2 Frac. A	238.3	36.7	1 SSC in 50 cells	1 SSC in 1846 cells
P8-9 Frac. A	669.2	17.2	1 SSC in 18 cells	1 SSC in 308 cells
P16-18 Frac. A	618.1	40.1	1 SSC in 19 cells	1 SSC in 779 cells

Table 5. SSC enrichment in Fraction A. Fold increase was calculated by comparing to data of unsorted cells in Table 3. Data for P8-9 Fraction A was compared to P6-8 data from Table 3. SSC frequency is the absolute number of SSCs assuming 12% homing efficiency (Nagano, 2003).

Age	**Method**	**Cell population**	**Colonies per 10^5 transplanted**	**Reference**
P8	Transgene	ID4-EGFP^{Bright}	~180	Helsel et al., 2017
P6	Transgene + FACS	ID4-EGFP^{+} TSPAN8^{High}	~240	Mutoji et al., 2016
P6	MACS	THY1+	228	Oatley et al., 2009
P4.5-7.5	MACS	THY1+	342	Kubota et al, 2004

Table 6. Notable previous studies with high levels of SSC enrichment from mouse pups.

Fraction A cells are incredibly efficient when used to establish SSC culture (Fig. 8B), even allowing culture initiation from the 129 mouse strain (Fig. 12), a strain that has been refractory to culture establishment in our lab. I also revealed that Fraction A is heterogeneous, with cells expressing transcripts of SSC, progenitor, and differentiation markers (Fig. 9), and could be further subfractionated using GFRA1 and KIT. I analyzed these subfractions with the transplantation assay and CFA, and their results glean new insights into spermatogonial development. It is not certain if this heterogeneity is beneficial or disadvantageous to cluster formation (or regeneration upon transplantation) and remains to be an interesting question to address in the future.

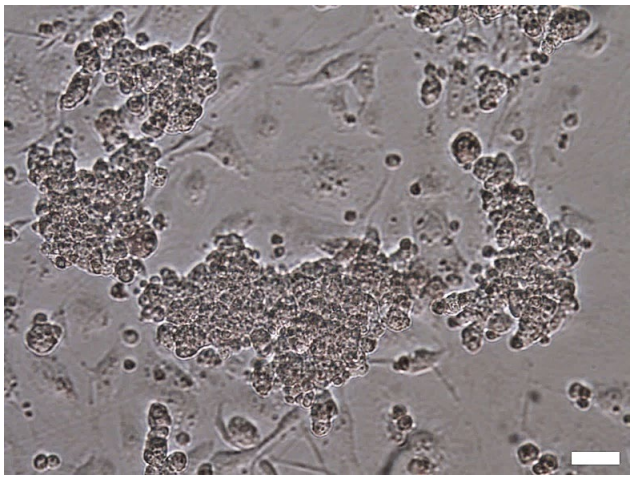

Figure 12. Clusters generated from P16 129 x 129ROSA pups (after five passages). Scale bar, 50 μm.

Although many SSC surface markers have been discovered (Table 1), the extensive fractionation of germ cell populations, as performed here, has not been common in the SSC field, compared to other stem cell and cancer research fields (particularly hematopoietic stem cells) which have more thoroughly characterized cell-surface antigen phenotypes (Lv et al., 2014; Seita and Weissman, 2010). To isolate pure SSCs, such an extensive fractionation will likely be needed, although a large number of SSC-specific markers may not be necessary (Kiel et al., 2005). For example, near-pure

HSCs were isolated using only three antigens that belong to the SLAM (Signaling Lymphocytic Activation Molecule) family receptors (Kiel et al., 2005).

Using markers THY1 and ITGA6, I found that Fraction A (THY1+ ITGA6+) contains all SSC activity in vivo and in vitro, regardless of prepubertal age in mice. Similar to our findings in adult testes, loss of either THY1 or ITGA6 led to a loss of all stem cell activity (Fig. 7B, 8A). Importantly, Fraction A cells can be used to generate long-term culture lines at all three developmental stages examined (P0-2, P8-9, and P16-18). Therefore, my study demonstrates a method of culture initiation that is more effective and versatile than the common method of THY1-based MACS. Using this new FACS-based method with negative selection of MHC-I, CD45, and CD74-expressing cells, I was able to culture 129 pup clusters long-term (Fig. 12), which was previously difficult due to the overgrowth of somatic cells.

By comparing long-term culture lines generated from different developmental stages, I found that while short-term cluster-forming activity varied greatly between ages (Fig. 8A), proliferative ability long-term was similar. My hypothesis is that short-term cluster-forming activity reflects the number of cluster-forming cells present in the initial cell population, which can be different from long-term proliferative activity. For instance, P8-9 Fraction A (334.5 ± 68.1 clusters per 10^5 cells seeded) had less short-term activity than P16-18 Fraction A (816.7 ± 174.1), so there were less cluster-forming cells present in the initial population. However, the long-term proliferative activity of P8-9 Fraction A was comparable (doubling time of 3.1 days versus 3.7 days for P16-18).

P0-2 Fraction A is a similar case, with lower short-term cluster-forming activity (101.5 clusters per 10^5 cells seeded) but long-term proliferative activity comparable to that seen at other developmental stages. What makes P0-2 clusters particularly interesting are the results of flow cytometric analyses. KIT expression in long-term clusters derived from P0-2 Fraction A is comparable to later developmental stages, which contrasts with the phenotype of P0-2 Fraction A in vivo where KIT expression is absent (Fig. 11). Thus, KIT expression emerges during culture, perhaps reflecting ongoing maturation of initial cells in the culture environment. KIT expression is accepted as a marker of spermatogonial differentiation in vivo, but the expression pattern of KIT in vitro does not

seem to reflect the same biological function as in vivo (Kanatsu-Shinohara et al., 2003; Morimoto et al., 2009). For instance, both the soluble (Kanatsu-Shinohara et al., 2003) and membrane-bound form (Morimoto et al., 2009) of KIT ligand seem to have no effect on proliferative activity in vitro when added to culture. Furthermore, adding KIT inhibitor ISCK03 or the KIT neutralizing antibody ACK2 did not affect proliferative activity in vitro (Morimoto et al., 2009). In summary, the biological function of KIT expression in vitro should be interpreted carefully.

In order to characterize SSC-enriched Fraction A at a higher resolution, I further subdivided Fraction A with GFRA1 and KIT, and found that almost all GFRA1/KIT subfractions retained SSC activity (Fig. 11). At P8-9, there was no further enrichment through GFRA1/KIT subfractionation as no subfractions exceeded 669.2 colonies per 10^5 cells transplanted (bulk Fraction A). But at P16-18, both the GFRA1+ KIT– and GFRA1+ KIT+ subfractions showed somewhat higher levels of SSC frequency (729.3 ± 84.8 and 744.2 ± 104.6 respectively) when compared to bulk Fraction A (618.1 ± 79.4). Overall, there could be a technical limitation in subdividing Fraction A with FACS to achieve higher levels of enrichment and attempts for high-resolution FACS might result in the loss of SSCs during multiple gating steps.

SSCs are commonly considered to be GFRA1+ and KIT–, but my data showed that both GFRA1– subfractions and KIT+ subfractions within Fraction A retained SSC activity. These somewhat counter-intuitive results are supported by many previous studies. Past fractionation studies have consistently shown GFRA1– cells to retain a considerable level of regeneration potential (Buageaw et al., 2005; Ebata et al., 2005; Garbuzov et al., 2018; Grisanti et al., 2009). These data indicate that GFRA1– cells have not progressed far along commitment such that all regenerative activity is lost.

One exception is P0-2, at which point the GFRA1– subfraction lacked regenerative activity at P0-2 and only the GFRA1+ subfraction possessed regenerative activity (282.8 ± 128.4 colonies per 10^5 cells transplanted). This data supports the idea of two different prospermatogonial subpopulations at birth. I suspect that the first wave of mouse spermatogenesis originates from the cells that belong to the GFRA1– fraction. An interesting observation is that the GFRA1– fraction at P0-2 exhibits some cluster-

forming potential, although lower than the GFRA1+ fraction. One possibility is that there is a cell population that can generate clusters in vitro but cannot regenerate spermatogenesis after transplantation. Further detailed analyses are required to test these hypotheses and possibilities.

Finally, my study raises some observations on spermatogonial commitment during postnatal development. Germ cells can be divided into two populations: Fraction A (THY1+ ITGA6+) and Fraction C (THY1– ITGA6^{mid}), the former being the SSC pool and the latter being SSC-depleted. Fraction C first appears at P8-9, and the germ cell population is roughly divided into one-half Fraction A (48.3%) and one-half Fraction C (50.7%). By P16-18, Fraction C has expanded in size considerably, comprising 83.3% of the germ cell population, while Fraction A comprises 12.1%. The rapid expansion of Fraction C can be attributed to three potential factors: 1) meiotic division of Fraction C cells, 2) mitotic division of Fraction C cells, and 3) commitment of Fraction A cells.

Expansion due to meiotic division should be low because by P16-18, spermatogenesis has progressed to the stage of round spermatid, and the number of secondary spermatocytes and round spermatids are negligible (Bellve et al., 1977; Janca et al., 1986). The first meiotic division occurs at the secondary spermatocyte stage, but the vast majority of germ cells are at the pachytene spermatocyte stage or earlier, so only a small amount of meiotic division should have occurred (Bellve et al., 1977; Janca et al., 1986). The second factor, mitotic division, should also be minimal in effect, as Fraction C cells have limited self-renewal activity in vitro (Fig. 8A) and regenerative activity in vivo (Fig. 7B). Thus, I attribute the rapid expansion of Fraction C to the third factor, commitment of Fraction A cells to form progenitors (Fraction C).

Examining the rapid expansion of Fraction C (14.9% of THY1/ITGA6 profile at P8-9 to 65.1% at P16-18), we can assume that Fraction A cells are producing progenitors at a high rate (Fig. 7D). In fact, I believe that the rate of progenitor production (Fraction C expansion) is higher than self-renewal (Fraction A expansion). Previously, it was reported that prepubertal SSCs differentiate more than they self-renew following transplantation (Ebata et al., 2007). Here, I present evidence for this phenomenon in intact prepubertal testes. One possible explanation is that because pup testes lack

mature germ cells, SSCs produce more progenitors as a compensatory mechanism, due to lack of cell signaling from mature germ cells. Another possible explanation is the altered endocrine environment in pup testes, such as higher levels of intratesticular testosterone (Jean-Faucher et al., 1978), although how exactly this would affect spermatogonial fate is unclear.

4.1 Limitations of Study

First, in sorting the cells with FACS, I cannot completely deny the possibility of contamination between subfractions, although the purity of FACS is known to be very high (Basu et al., 2010).

Second, while THY1/ITGA6 fractionation was very efficient in SSC purification, GFRA1/KIT subfractionation led to stem cell loss. Fraction A cells at P8-9 when transplanted produced 669.2 ± 69.0 colonies per 10^5 cells transplanted, but none of its subfractions exceeded this level. Stem cell loss from FACS has been documented in the SSC field (Shinohara et al., 2000) as well as other fields (Britt et al., 2009; Hunt, 1979). Some potential causes are the removal of committed progenitors which support regenerative activity and blocking surface protein function with fluorescent antibodies (Alexander et al., 2009). In our unpublished data, further fractionating adult THY1+ ITGA6+ cells with other markers like CDH1 and MCAM similarly lead to stem cell loss.

Third, the CFA results show a lot of variability (high SD/SEM in Fig. 11C). Some possible causes could be variability in medium batch and STO feeder batch, both of which can affect the number of clusters formed.

4.2 Future direction

First, I focused on germ cells in this study and did not characterize somatic cell fractions in THY1/ITGA6 profiles (Fig. 6D). It could be interesting to describe the various types of testis somatic cells (e.g. Sertoli, Leydig, stromal, endothelial, and blood cells).

Second, it would be interesting to conduct lineage tracing and live imaging studies to study THY1+ and THY1– cells. It could be interesting to examine if there is reversibility (i.e. dedifferentiation) in THY1+ and THY1– populations like there is for GFRA1+ and NGN3+ cells (Nakagawa et al., 2010).

Third, transcriptional profiling of GFRA1/KIT subfractions can be done. Unlike THY1/ITGA6 subfractions, I was not able to examine GFRA1/KIT subfractions at the transcript level. In addition, scRNA-seq of Fractions A and C could be beneficial in characterizing the heterogeneous populations in each fraction, and pseudotiming analyses could be conducted to examine potential commitment processes.

Fourth, our fractionation experiments can be extended to prenatal periods, particularly at E14.5, a period at which germ cells can efficiently regenerate spermatogenesis (Chuma et al., 2005), and which no fractionation of germ cells has been reported so far. Here, it may be possible to subfractionate the germ cell population based on GFRA1 expression like P0-2 Fraction A and analyze subfractions with the transplantation assay and CFA.

Finally, my mouse study can be used as a model for the study of human SSC development and establishment. It should provide essential information to understand the postnatal SSC development in other mammalian species, including humans.

5. References

Alexander, C.M., Puchalski, J., Klos, K.S., Badders, N., Ailles, L., Kim, C.F., Dirks, P., Smalley, M.J., 2009. Separating Stem Cells by Flow Cytometry: Reducing Variability for Solid Tissues. Cell Stem Cell 5, 579–583. https://doi.org/10.1016/j.stem.2009.11.008

Amann, R.P., 2009. Considerations in Evaluating Human Spermatogenesis on the Basis of Total Sperm per Ejaculate. Journal of Andrology 30, 626–641. https://doi.org/10.2164/jandrol.108.006817

Avalos, A.M., Valdivia, A.D., Muñoz, N., Herrera-Molina, R., Tapia, J.C., Lavandero, S., Chiong, M., Burridge, K., Schneider, P., Quest, A.F.G., Leyton, L., 2009. Neuronal Thy-1 induces astrocyte adhesion by engaging syndecan-4 in a cooperative interaction with αvβ3 integrin that activates PKCα and RhoA. Journal of Cell Science 122, 3462–3471. https://doi.org/10.1242/jcs.034827

Barlow, J.Z., Kelley, K.A., Bozdagi, O., Huntley, G.W., 2002. Testing the role of the cell-surface molecule Thy-1 in regeneration and plasticity of connectivity in the CNS. Neuroscience 111, 837–852. https://doi.org/10.1016/S0306-4522(02)00023-4

Barroca, V., Lassalle, B., Coureuil, M., Louis, J.P., Le Page, F., Testart, J., Allemand, I., Riou, L., Fouchet, P., 2009. Mouse differentiating spermatogonia can generate germinal stem cells in vivo. Nat Cell Biol 11, 190–196. https://doi.org/10.1038/ncb1826

Bashamboo, A., Taylor, A.H., Samuel, K., Panthier, J.-J., Whetton, A.D., Forrester, L.M., 2006. The survival of differentiating embryonic stem cells is dependent on the SCF-KIT pathway. Journal of Cell Science 119, 3039–3046. https://doi.org/10.1242/jcs.03038

Basu, S., Campbell, H.M., Dittel, B.N., Ray, A., 2010. Purification of Specific Cell Population by Fluorescence Activated Cell Sorting (FACS). J Vis Exp 1546. https://doi.org/10.3791/1546

Beamer, W.G., Cunliffe-Beamer, T.L., Shultz, K.L., Langley, S.H., Roderick, T.H., 1988. Juvenile Spermatogonial Depletion (jsd): A Genetic Defect of Germ Cell Proliferation of Male Mice1. Biology of Reproduction 38, 899–908. https://doi.org/10.1095/biolreprod38.4.899

Bellve, A., Cavicchia, J., Millette, C., O'Brien, D., Bhatnagar, Y., Dym, M., 1977. Spermatogenic cells of the prepuberal mouse: isolation and morphological characterization. Journal of Cell Biology 74, 68–85. https://doi.org/10.1083/jcb.74.1.68

Brinster, R.L., Avarbock, M.R., 1994. Germline transmission of donor haplotype following spermatogonial transplantation. Proceedings of the National Academy of Sciences 91, 11303–11307. https://doi.org/10.1073/pnas.91.24.11303

Brinster, R.L., Zimmermann, J.W., 1994. Spermatogenesis following male germ-cell transplantation. Proceedings of the National Academy of Sciences 91, 11298–11302. https://doi.org/10.1073/pnas.91.24.11298

Britt, K.L., Kendrick, H., Regan, J.L., Molyneux, G., Magnay, F.-A., Ashworth, A., Smalley, M.J., 2009. Pregnancy in the mature adult mouse does not alter the

proportion of mammary epithelial stem/progenitor cells. Breast Cancer Research 11, R20. https://doi.org/10.1186/bcr2245
Buageaw, A., Sukhwani, M., Ben-Yehudah, A., Ehmcke, J., Rawe, V.Y., Pholpramool, C., Orwig, K.E., Schlatt, S., 2005. GDNF Family Receptor alpha1 Phenotype of Spermatogonial Stem Cells in Immature Mouse Testes1. Biology of Reproduction 73, 1011–1016. https://doi.org/10.1095/biolreprod.105.043810
Busada, J.T., Kaye, E.P., Renegar, R.H., Geyer, C.B., 2014. Retinoic Acid Induces Multiple Hallmarks of the Prospermatogonia-to-Spermatogonia Transition in the Neonatal Mouse1. Biology of Reproduction 90, 64, 1–11. https://doi.org/10.1095/biolreprod.113.114645
Cacalano, G., Fariñas, I., Wang, L.-C., Hagler, K., Forgie, A., Moore, M., Armanini, M., Phillips, H., Ryan, A.M., Reichardt, L.F., Hynes, M., Davies, A., Rosenthal, A., 1998. GFRα1 Is an Essential Receptor Component for GDNF in the Developing Nervous System and Kidney. Neuron 21, 53–62. https://doi.org/10.1016/S0896-6273(00)80514-0
Campbell, I.D., Humphries, M.J., 2011. Integrin Structure, Activation, and Interactions. Cold Spring Harb Perspect Biol 3, a004994. https://doi.org/10.1101/cshperspect.a004994
Chan, F., Oatley, M.J., Kaucher, A.V., Yang, Q.-E., Bieberich, C.J., Shashikant, C.S., Oatley, J.M., 2014. Functional and molecular features of the Id4+ germline stem cell population in mouse testes. Genes Dev 28, 1351–1362. https://doi.org/10.1101/gad.240465.114
Chen, H., Mruk, D., Xiao, X., Cheng, C.Y., 2017. Human Spermatogenesis and Its Regulation, in: Winters, S.J., Huhtaniemi, I.T. (Eds.), Male Hypogonadism: Basic, Clinical and Therapeutic Principles, Contemporary Endocrinology. Springer International Publishing, Cham, pp. 49–72. https://doi.org/10.1007/978-3-319-53298-1_3
Chen, L.-Y., Willis, W.D., Eddy, E.M., 2016. Targeting the Gdnf Gene in peritubular myoid cells disrupts undifferentiated spermatogonial cell development. Proceedings of the National Academy of Sciences 113, 1829–1834. https://doi.org/10.1073/pnas.1517994113
Chen, M., Cen, C., Wang, N., Shen, Z., Wang, M., Liu, B., Li, J., Cui, X., Wang, Y., Gao, F., 2022. The functions of Wt1 in mouse gonad development and somatic cells differentiation†. Biology of Reproduction 107, 269–274. https://doi.org/10.1093/biolre/ioac050
Chihara, M., Otsuka, S., Ichii, O., Kon, Y., 2013. Vitamin A Deprivation Affects the Progression of the Spermatogenic Wave and Initial Formation of the Blood-testis Barrier, Resulting in Irreversible Testicular Degeneration in Mice. Journal of Reproduction and Development 59, 525–535. https://doi.org/10.1262/jrd.2013-058
Chuma, S., Kanatsu-Shinohara, M., Inoue, K., Ogonuki, N., Miki, H., Toyokuni, S., Hosokawa, M., Nakatsuji, N., Ogura, A., Shinohara, T., 2005. Spermatogenesis from epiblast and primordial germ cells following transplantation into postnatal mouse testis. Development 132, 117–122. https://doi.org/10.1242/dev.01555

Clermont, Y., 1972. Kinetics of spermatogenesis in mammals: seminiferous epithelium cycle and spermatogonial renewal. Physiological Reviews 52, 198–236. https://doi.org/10.1152/physrev.1972.52.1.198
Costoya, J.A., Hobbs, R.M., Barna, M., Cattoretti, G., Manova, K., Sukhwani, M., Orwig, K.E., Wolgemuth, D.J., Pandolfi, P.P., 2004. Essential role of Plzf in maintenance of spermatogonial stem cells. Nat Genet 36, 653–659. https://doi.org/10.1038/ng1367
Culty, M., 2009. Gonocytes, the forgotten cells of the germ cell lineage. Birth Defects Research Part C: Embryo Today: Reviews 87, 1–26. https://doi.org/10.1002/bdrc.20142
de Rooij, D.G., 2017. Organization of the Seminiferous Epithelium and the Cycle, and Morphometric Description of Spermatogonial Subtypes (Rodents and Primates), in: Oatley, J.M., Griswold, M.D. (Eds.), The Biology of Mammalian Spermatogonia. Springer, New York, NY, pp. 3–20. https://doi.org/10.1007/978-1-4939-7505-1_1
de Rooij, D.G., 1998. Stem cells in the testis. Int J Exp Pathol 79, 67–80. https://doi.org/10.1046/j.1365-2613.1998.00057.x
Draper, J.S., Pigott, C., Thomson, J.A., Andrews, P.W., 2002. Surface antigens of human embryonic stem cells: changes upon differentiation in culture*. Journal of Anatomy 200, 249–258. https://doi.org/10.1046/j.1469-7580.2002.00030.x
D'Souza, S.E., Ginsberg, M.H., Plow, E.F., 1991. Arginyl-glycyl-aspartic acid (RGD): a cell adhesion motif. Trends in Biochemical Sciences 16, 246–250. https://doi.org/10.1016/0968-0004(91)90096-E
Ebata, K.T., Zhang, X., Nagano, M.C., 2007. Male Germ Line Stem Cells Have an Altered Potential to Proliferate and Differentiate During Postnatal Development in Mice1. Biology of Reproduction 76, 841–847. https://doi.org/10.1095/biolreprod.106.058305
Ebata, K.T., Zhang, X., Nagano, M.C., 2005. Expression patterns of cell-surface molecules on male germ line stem cells during postnatal mouse development. Molecular Reproduction and Development 72, 171–181. https://doi.org/10.1002/mrd.20324
Fiore, V.F., Ju, L., Chen, Y., Zhu, C., Barker, T.H., 2014. Dynamic catch of a Thy-1–α5β1+syndecan-4 trimolecular complex. Nat Commun 5, 4886. https://doi.org/10.1038/ncomms5886
França, L.R., Hess, R.A., Dufour, J.M., Hofmann, M.C., Griswold, M.D., 2016. The Sertoli cell: one hundred fifty years of beauty and plasticity. Andrology 4, 189–212. https://doi.org/10.1111/andr.12165
Friedrich, G., Soriano, P., 1991. Promoter traps in embryonic stem cells: a genetic screen to identify and mutate developmental genes in mice. Genes Dev. 5, 1513–1523. https://doi.org/10.1101/gad.5.9.1513
Garbuzov, A., Pech, M.F., Hasegawa, K., Sukhwani, M., Zhang, R.J., Orwig, K.E., Artandi, S.E., 2018. Purification of GFRα1+ and GFRα1– Spermatogonial Stem Cells Reveals a Niche-Dependent Mechanism for Fate Determination. Stem Cell Reports 10, 553–567. https://doi.org/10.1016/j.stemcr.2017.12.009
Geyer, C.B., 2017. Setting the Stage: The First Round of Spermatogenesis, in: Oatley, J.M., Griswold, M.D. (Eds.), The Biology of Mammalian Spermatogonia.

Springer, New York, NY, pp. 39–63. https://doi.org/10.1007/978-1-4939-7505-1_3
Givelet, M., Firlej, V., Lassalle, B., Gille, A.S., Lapoujade, C., Holtzman, I., Jarysta, A., Haghighirad, F., Dumont, F., Jacques, S., Letourneur, F., Pflumio, F., Allemand, I., Patrat, C., Thiounn, N., Wolf, J.P., Riou, L., Barraud-Lange, V., Fouchet, P., 2022. Transcriptional profiling of β-2M−SPα-6+THY1+ spermatogonial stem cells in human spermatogenesis. Stem Cell Reports 17, 936–952. https://doi.org/10.1016/j.stemcr.2022.02.017
Grasso, M., Fuso, A., Dovere, L., Rooij, D.G. de, Stefanini, M., Boitani, C., Vicini, E., 2012. Distribution of GFRA1-expressing spermatogonia in adult mouse testis. Reproduction 143, 325–332. https://doi.org/10.1530/REP-11-0385
Green, C.D., Ma, Q., Manske, G.L., Shami, A.N., Zheng, X., Marini, S., Moritz, L., Sultan, C., Gurczynski, S.J., Moore, B.B., Tallquist, M.D., Li, J.Z., Hammoud, S.S., 2018. A Comprehensive Roadmap of Murine Spermatogenesis Defined by Single-Cell RNA-Seq. Developmental Cell 46, 651-667.e10. https://doi.org/10.1016/j.devcel.2018.07.025
Grisanti, L., Falciatori, I., Grasso, M., Dovere, L., Fera, S., Muciaccia, B., Fuso, A., Berno, V., Boitani, C., Stefanini, M., Vicini, E., 2009. Identification of Spermatogonial Stem Cell Subsets by Morphological Analysis and Prospective Isolation. Stem Cells 27, 3043–3052. https://doi.org/10.1002/stem.206
Griswold, M.D., 2016. Spermatogenesis: The Commitment to Meiosis. Physiological Reviews 96, 1–17. https://doi.org/10.1152/physrev.00013.2015
Guo, J., Grow, E.J., Yi, C., Mlcochova, H., Maher, G.J., Lindskog, C., Murphy, P.J., Wike, C.L., Carrell, D.T., Goriely, A., Hotaling, J.M., Cairns, B.R., 2017. Chromatin and Single-Cell RNA-Seq Profiling Reveal Dynamic Signaling and Metabolic Transitions during Human Spermatogonial Stem Cell Development. Cell Stem Cell 21, 533-546.e6. https://doi.org/10.1016/j.stem.2017.09.003
Guo, J.U., Su, Y., Shin, J.H., Shin, J., Li, H., Xie, B., Zhong, C., Hu, S., Le, T., Fan, G., Zhu, H., Chang, Q., Gao, Y., Ming, G., Song, H., 2014. Distribution, recognition and regulation of non-CpG methylation in the adult mammalian brain. Nat Neurosci 17, 215–222. https://doi.org/10.1038/nn.3607
Hajkova, P., Erhardt, S., Lane, N., Haaf, T., El-Maarri, O., Reik, W., Walter, J., Surani, M.A., 2002. Epigenetic reprogramming in mouse primordial germ cells. Mechanisms of Development 117, 15–23. https://doi.org/10.1016/S0925-4773(02)00181-8
Hayashi, K., de Sousa Lopes, S.M.C., Surani, M.A., 2007. Germ Cell Specification in Mice. Science 316, 394–396. https://doi.org/10.1126/science.1137545
He, Z., Kokkinaki, M., Jiang, J., Zeng, W., Dobrinski, I., Dym, M., 2012. Isolation of Human Male Germ-Line Stem Cells Using Enzymatic Digestion and Magnetic-Activated Cell Sorting. Methods Mol Biol 825, 45–57. https://doi.org/10.1007/978-1-61779-436-0_4
Helsel, A.R., Yang, Q.-E., Oatley, M.J., Lord, T., Sablitzky, F., Oatley, J.M., 2017. ID4 levels dictate the stem cell state in mouse spermatogonia. Development 144, 624–634. https://doi.org/10.1242/dev.146928
Hermann, B.P., Cheng, K., Singh, A., Roa-De La Cruz, L., Mutoji, K.N., Chen, I.-C., Gildersleeve, H., Lehle, J.D., Mayo, M., Westernströer, B., Law, N.C., Oatley,

M.J., Velte, E.K., Niedenberger, B.A., Fritze, D., Silber, S., Geyer, C.B., Oatley, J.M., McCarrey, J.R., 2018. The Mammalian Spermatogenesis Single-Cell Transcriptome, from Spermatogonial Stem Cells to Spermatids. Cell Reports 25, 1650-1667.e8. https://doi.org/10.1016/j.celrep.2018.10.026
Hermann, B.P., Mutoji, K.N., Velte, E.K., Ko, D., Oatley, J.M., Geyer, C.B., McCarrey, J.R., 2015. Transcriptional and Translational Heterogeneity among Neonatal Mouse Spermatogonia1. Biology of Reproduction 92, 54, 1–12. https://doi.org/10.1095/biolreprod.114.125757
Hofmann, M.-C., Braydich-Stolle, L., Dym, M., 2005. Isolation of male germ-line stem cells; influence of GDNF. Developmental Biology 279, 114–124. https://doi.org/10.1016/j.ydbio.2004.12.006
Hu, Y.-C., de Rooij, D.G., Page, D.C., 2013. Tumor suppressor gene Rb is required for self-renewal of spermatogonial stem cells in mice. Proceedings of the National Academy of Sciences 110, 12685–12690. https://doi.org/10.1073/pnas.1311548110
Huckins, C., Oakberg, E.F., 1978. Morphological and quantitative analysis of spermatogonia in mouse testes using whole mounted seminiferous tubules. I. The normal testes. The Anatomical Record 192, 519–527. https://doi.org/10.1002/ar.1091920406
Hunt, S.V., 1979. The presence of Thy-1 on the surface of rat lymphoid stem cells and colony-forming units. European Journal of Immunology 9, 853–859. https://doi.org/10.1002/eji.1830091105
Janca, F.C., Jost, L.K., Evenson, D.P., 1986. Mouse Testicular and Sperm Cell Development Characterized from Birth to Adulthood by Dual Parameter Flow Cytometry1. Biology of Reproduction 34, 613–623. https://doi.org/10.1095/biolreprod34.4.613
Jean-Faucher, Ch., Berger, M., de Turckheim, M., Veyssiere, G., Jean, Cl., 1978. DEVELOPMENTAL PATTERNS OF PLASMA AND TESTICULAR TESTOSTERONE IN MICE FROM BIRTH TO ADULTHOOD. Acta Endocrinologica (Norway) 89, 780–788. https://doi.org/10.1530/acta.0.0890780
Jégou, B., 1992. 3 The sertoli cell. Baillière's Clinical Endocrinology and Metabolism, The Testes 6, 273–311. https://doi.org/10.1016/S0950-351X(05)80151-X
Kanatsu-Shinohara, M., Inoue, K., Miki, H., Ogonuki, N., Takehashi, M., Morimoto, T., Ogura, A., Shinohara, T., 2006. Clonal Origin of Germ Cell Colonies after Spermatogonial Transplantation in Mice1. Biology of Reproduction 75, 68–74. https://doi.org/10.1095/biolreprod.106.051193
Kanatsu-Shinohara, M., Morimoto, H., Shinohara, T., 2012. Enrichment of Mouse Spermatogonial Stem Cells by Melanoma Cell Adhesion Molecule Expression1. Biology of Reproduction 87, 139, 1–10. https://doi.org/10.1095/biolreprod.112.103861
Kanatsu-Shinohara, M., Ogonuki, N., Inoue, K., Miki, H., Ogura, A., Toyokuni, S., Shinohara, T., 2003. Long-Term Proliferation in Culture and Germline Transmission of Mouse Male Germline Stem Cells1. Biology of Reproduction 69, 612–616. https://doi.org/10.1095/biolreprod.103.017012
Kanatsu-Shinohara, M., Ogonuki, N., Iwano, T., Lee, J., Kazuki, Y., Inoue, K., Miki, H., Takehashi, M., Toyokuni, S., Shinkai, Y., Oshimura, M., Ishino, F., Ogura, A.,

Shinohara, T., 2005. Genetic and epigenetic properties of mouse male germline stem cells during long-term culture. Development 132, 4155–4163. https://doi.org/10.1242/dev.02004
Kanatsu-Shinohara, M., Takashima, S., Ishii, K., Shinohara, T., 2011. Dynamic Changes in EPCAM Expression during Spermatogonial Stem Cell Differentiation in the Mouse Testis. PLOS ONE 6, e23663. https://doi.org/10.1371/journal.pone.0023663
Kanatsu-Shinohara, M., Toyokuni, S., Shinohara, T., 2004. CD9 Is a Surface Marker on Mouse and Rat Male Germline Stem Cells1. Biology of Reproduction 70, 70–75. https://doi.org/10.1095/biolreprod.103.020867
Kawai, K., Takahashi, M., 2020. Intracellular RET signaling pathways activated by GDNF. Cell Tissue Res 382, 113–123. https://doi.org/10.1007/s00441-020-03262-1
Kiel, M.J., Yilmaz, Ö.H., Iwashita, T., Yilmaz, O.H., Terhorst, C., Morrison, S.J., 2005. SLAM Family Receptors Distinguish Hematopoietic Stem and Progenitor Cells and Reveal Endothelial Niches for Stem Cells. Cell 121, 1109–1121. https://doi.org/10.1016/j.cell.2005.05.026
Kluin, Ph.M., Kramer, M.F., de Rooij, D.G., 1982. Spermatogenesis in the immature mouse proceeds faster than in the adult. International Journal of Andrology 5, 282–294. https://doi.org/10.1111/j.1365-2605.1982.tb00257.x
Kong, M., Muñoz, N., Valdivia, A., Alvarez, A., Herrera-Molina, R., Cárdenas, A., Schneider, P., Burridge, K., Quest, A.F.G., Leyton, L., 2013. Thy-1-mediated cell–cell contact induces astrocyte migration through the engagement of αVβ3 integrin and syndecan-4. Biochimica et Biophysica Acta (BBA) - Molecular Cell Research 1833, 1409–1420. https://doi.org/10.1016/j.bbamcr.2013.02.013
Kubo, N., Toh, H., Shirane, K., Shirakawa, T., Kobayashi, H., Sato, T., Sone, H., Sato, Y., Tomizawa, S., Tsurusaki, Y., Shibata, H., Saitsu, H., Suzuki, Y., Matsumoto, N., Suyama, M., Kono, T., Ohbo, K., Sasaki, H., 2015. DNA methylation and gene expression dynamics during spermatogonial stem cell differentiation in the early postnatal mouse testis. BMC Genomics 16, 624. https://doi.org/10.1186/s12864-015-1833-5
Kubota, H., Avarbock, M.R., Brinster, R.L., 2004. Growth factors essential for self-renewal and expansion of mouse spermatogonial stem cells. Proceedings of the National Academy of Sciences 101, 16489–16494. https://doi.org/10.1073/pnas.0407063101
Kubota, H., Avarbock, M.R., Brinster, R.L., 2003. Spermatogonial stem cells share some, but not all, phenotypic and functional characteristics with other stem cells. Proceedings of the National Academy of Sciences 100, 6487–6492. https://doi.org/10.1073/pnas.0631767100
Kumar, A., Bhanja, A., Bhattacharyya, J., Jaganathan, B.G., 2016. Multiple roles of CD90 in cancer. Tumor Biol. 37, 11611–11622. https://doi.org/10.1007/s13277-016-5112-0
La, H.M., Mäkelä, J.-A., Chan, A.-L., Rossello, F.J., Nefzger, C.M., Legrand, J.M.D., De Seram, M., Polo, J.M., Hobbs, R.M., 2018. Identification of dynamic undifferentiated cell states within the male germline. Nat Commun 9, 2819. https://doi.org/10.1038/s41467-018-04827-z

Law, N.C., Oatley, M.J., Oatley, J.M., 2019. Developmental kinetics and transcriptome dynamics of stem cell specification in the spermatogenic lineage. Nat Commun 10, 2787. https://doi.org/10.1038/s41467-019-10596-0

Leyton, L., Schneider, P., Labra, C.V., Rüegg, C., Hetz, C.A., Quest, A.F.G., Bron, C., 2001. Thy-1 binds to integrin β3 on astrocytes and triggers formation of focal contact sites. Current Biology 11, 1028–1038. https://doi.org/10.1016/S0960-9822(01)00262-7

Liao, J., Ng, S.H., Luk, A.C., Suen, H.C., Qian, Y., Lee, A.W.T., Tu, J., Fung, J.C.L., Tang, N.L.S., Feng, B., Chan, W.Y., Fouchet, P., Hobbs, R.M., Lee, T.L., 2019. Revealing cellular and molecular transitions in neonatal germ cell differentiation using single cell RNA sequencing. Development 146, dev174953. https://doi.org/10.1242/dev.174953

Lim, J.J., Sung, S.-Y., Kim, H.J., Song, S.-H., Hong, J.Y., Yoon, T.K., Kim, J.K., Kim, K.-S., Lee, D.R., 2010. Long-term proliferation and characterization of human spermatogonial stem cells obtained from obstructive and non-obstructive azoospermia under exogenous feeder-free culture conditions. Cell Proliferation 43, 405–417. https://doi.org/10.1111/j.1365-2184.2010.00691.x

Liu, S., Tang, Z., Xiong, T., Tang, W., 2011. Isolation and characterization of human spermatogonial stem cells. Reprod Biol Endocrinol 9, 141. https://doi.org/10.1186/1477-7827-9-141

Lovelace, D.L., Gao, Z., Mutoji, K., Song, Y.C., Ruan, J., Hermann, B.P., 2016. The regulatory repertoire of PLZF and SALL4 in undifferentiated spermatogonia. Development 143, 1893–1906. https://doi.org/10.1242/dev.132761

Lv, F.-J., Tuan, R.S., Cheung, K.M.C., Leung, V.Y.L., 2014. Concise Review: The Surface Markers and Identity of Human Mesenchymal Stem Cells. Stem Cells 32, 1408–1419. https://doi.org/10.1002/stem.1681

Main, A.L., Harvey, T.S., Baron, M., Boyd, J., Campbell, I.D., 1992. The three-dimensional structure of the tenth type III module of fibronectin: An insight into RGD-mediated interactions. Cell 71, 671–678. https://doi.org/10.1016/0092-8674(92)90600-H

Makino, Y., Jensen, N.H., Yokota, N., Rossner, M.J., Akiyama, H., Shirahige, K., Okada, Y., 2019. Single cell RNA-sequencing identified Dec2 as a suppressive factor for spermatogonial differentiation by inhibiting Sohlh1 expression. Sci Rep 9, 6063. https://doi.org/10.1038/s41598-019-42578-z

McCarrey, J.R., 2017. Transition of Prenatal Prospermatogonia to Postnatal Spermatogonia, in: Oatley, J.M., Griswold, M.D. (Eds.), The Biology of Mammalian Spermatogonia. Springer, New York, NY, pp. 23–38. https://doi.org/10.1007/978-1-4939-7505-1_2

Medrano, J.V., Rombaut, C., Simon, C., Pellicer, A., Goossens, E., 2016. Human spermatogonial stem cells display limited proliferation in vitro under mouse spermatogonial stem cell culture conditions. Fertility and Sterility 106, 1539-1549.e8. https://doi.org/10.1016/j.fertnstert.2016.07.1065

Miki, H., Lee, J., Inoue, K., Ogonuki, N., Noguchi, Y., Mochida, K., Kohda, T., Nagashima, H., Ishino, F., Ogura, A., 2004. Microinsemination with First-Wave Round Spermatids from Immature Male Mice. Journal of Reproduction and Development 50, 131–137. https://doi.org/10.1262/jrd.50.131

Mintz, B., Russell, E.S., 1957. Gene-induced embryological modifications of primordial germ cells in the mouse. Journal of Experimental Zoology 134, 207–237. https://doi.org/10.1002/jez.1401340202
Mori, C., Nakamura, N., Dix, D.J., Fujioka, M., Nakagawa, S., Shiota, K., Eddy, E.M., 1997. Morphological analysis of germ cell apoptosis during postnatal testis development in normal and Hsp70-2 knockout mice. Developmental Dynamics 208, 125–136. https://doi.org/10.1002/(SICI)1097-0177(199701)208:1<125::AID-AJA12>3.0.CO;2-5
Morimoto, H., Kanastu-Shinohara, M., Ogonuki, N., Kamimura, S., Ogura, A., Yabe-Nishimura, C., Mori, Y., Morimoto, T., Watanabe, S., Otsu, K., Yamamoto, T., Shinohara, T., 2019. ROS amplification drives mouse spermatogonial stem cell self-renewal. Life Science Alliance 2. https://doi.org/10.26508/lsa.201900374
Morimoto, H., Kanatsu-Shinohara, M., Orwig, K.E., Shinohara, T., 2020. Expression and functional analyses of ephrin type-A receptor 2 in mouse spermatogonial stem cells. Biology of Reproduction 102, 220. https://doi.org/10.1093/biolre/ioz156
Morimoto, H., Kanatsu-Shinohara, M., Takashima, S., Chuma, S., Nakatsuji, N., Takehashi, M., Shinohara, T., 2009. Phenotypic Plasticity of Mouse Spermatogonial Stem Cells. PLOS ONE 4, e7909. https://doi.org/10.1371/journal.pone.0007909
Motro, B., Bernstein, A., 1993. Dynamic changes in ovarian c-kit and Steel expression during the estrous reproductive cycle. Developmental Dynamics 197, 69–79. https://doi.org/10.1002/aja.1001970107
Mruk, D.D., Cheng, C.Y., 2015. The Mammalian Blood-Testis Barrier: Its Biology and Regulation. Endocrine Reviews 36, 564–591. https://doi.org/10.1210/er.2014-1101
Mutoji, K., Singh, A., Nguyen, T., Gildersleeve, H., Kaucher, A.V., Oatley, M.J., Oatley, J.M., Velte, E.K., Geyer, C.B., Cheng, K., McCarrey, J.R., Hermann, B.P., 2016. TSPAN8 Expression Distinguishes Spermatogonial Stem Cells in the Prepubertal Mouse Testis1. Biology of Reproduction 95, 117, 1–14. https://doi.org/10.1095/biolreprod.116.144220
Nagano, M., Avarbock, M.R., Brinster, R.L., 1999. Pattern and Kinetics of Mouse Donor Spermatogonial Stem Cell Colonization in Recipient Testes1. Biology of Reproduction 60, 1429–1436. https://doi.org/10.1095/biolreprod60.6.1429
Nagano, M., Brinster, C.J., Orwig, K.E., Ryu, B.-Y., Avarbock, M.R., Brinster, R.L., 2001. Transgenic mice produced by retroviral transduction of male germ-line stem cells. Proceedings of the National Academy of Sciences 98, 13090–13095. https://doi.org/10.1073/pnas.231473498
Nagano, M., Patrizio, P., Brinster, R.L., 2002a. Long-term survival of human spermatogonial stem cells in mouse testes. Fertility and Sterility 78, 1225–1233. https://doi.org/10.1016/S0015-0282(02)04345-5
Nagano, M., Ryu, B.-Y., Brinster, C.J., Avarbock, M.R., Brinster, R.L., 2003. Maintenance of Mouse Male Germ Line Stem Cells In Vitro1. Biology of Reproduction 68, 2207–2214. https://doi.org/10.1095/biolreprod.102.014050
Nagano, M., Watson, D.J., Ryu, B.-Y., Wolfe, J.H., Brinster, R.L., 2002b. Lentiviral vector transduction of male germ line stem cells in mice. FEBS Letters 524, 111–115. https://doi.org/10.1016/S0014-5793(02)03010-7

Nagano, M.C., 2003. Homing Efficiency and Proliferation Kinetics of Male Germ Line Stem Cells Following Transplantation in Mice1. Biology of Reproduction 69, 701–707. https://doi.org/10.1095/biolreprod.103.016352
Nakagawa, T., Sharma, M., Nabeshima, Y., Braun, R.E., Yoshida, S., 2010. Functional Hierarchy and Reversibility Within the Murine Spermatogenic Stem Cell Compartment. Science 328, 62–67. https://doi.org/10.1126/science.1182868
Nickkholgh, B., Mizrak, S.C., Korver, C.M., van Daalen, S.K.M., Meissner, A., Repping, S., van Pelt, A.M.M., 2014. Enrichment of spermatogonial stem cells from long-term cultured human testicular cells. Fertility and Sterility 102, 558-565.e5. https://doi.org/10.1016/j.fertnstert.2014.04.022
Niedenberger, B.A., Busada, J.T., Geyer, C.B., 2015. Marker expression reveals heterogeneity of spermatogonia in the neonatal mouse testis. Reproduction 149, 329–338. https://doi.org/10.1530/REP-14-0653
Nosten-Bertrand, M., Errington, M.L., Murphy, K.P.S.J., Tokugawa, Y., Barboni, E., Kozlova, E., Michalovich, D., Morris, R.G.M., Silver, J., Stewart, C.L., Bliss, T.V.P., Morris, R.J., 1996. Normal spatial learning despite regional inhibition of LTP in mice lacking Thy-1. Nature 379, 826–829. https://doi.org/10.1038/379826a0
Oatley, J.M., Oatley, M.J., Avarbock, M.R., Tobias, J.W., Brinster, R.L., 2009. Colony stimulating factor 1 is an extrinsic stimulator of mouse spermatogonial stem cell self-renewal. Development 136, 1191–1199. https://doi.org/10.1242/dev.032243
Ohbo, K., Yoshida, S., Ohmura, M., Ohneda, O., Ogawa, T., Tsuchiya, H., Kuwana, T., Kehler, J., Abe, K., Schöler, H.R., Suda, T., 2003. Identification and characterization of stem cells in prepubertal spermatogenesis in mice. Developmental Biology 258, 209–225. https://doi.org/10.1016/S0012-1606(03)00111-8
Ohinata, Y., Ohta, H., Shigeta, M., Yamanaka, K., Wakayama, T., Saitou, M., 2009. A Signaling Principle for the Specification of the Germ Cell Lineage in Mice. Cell 137, 571–584. https://doi.org/10.1016/j.cell.2009.03.014
Ohta, H., Tohda, A., Nishimune, Y., 2003. Proliferation and Differentiation of Spermatogonial Stem Cells in the W/Wv Mutant Mouse Testis1. Biology of Reproduction 69, 1815–1821. https://doi.org/10.1095/biolreprod.103.019323
Ohta, H., Wakayama, T., Nishimune, Y., 2004. Commitment of Fetal Male Germ Cells to Spermatogonial Stem Cells During Mouse Embryonic Development1. Biology of Reproduction 70, 1286–1291. https://doi.org/10.1095/biolreprod.103.024612
Peng, Y.J., Tang, X.T., Shu, H.S., Dong, W., Shao, H., Zhou, B.O., 2023. Sertoli cells are the source of stem cell factor for spermatogenesis. Development 150, dev200706. https://doi.org/10.1242/dev.200706
Raivo Kolde, 2019. pheatmap: Pretty Heatmaps.
Richardson, B.E., Lehmann, R., 2010. Mechanisms guiding primordial germ cell migration: strategies from different organisms. Nat Rev Mol Cell Biol 11, 37–49. https://doi.org/10.1038/nrm2815
Saalbach, A., Wetzel, A., Haustein, U.-F., Sticherling, M., Simon, J.C., Anderegg, U., 2005. Interaction of human Thy-1 (CD 90) with the integrin αvβ3 (CD51/CD61): an important mechanism mediating melanoma cell adhesion to activated endothelium. Oncogene 24, 4710–4720. https://doi.org/10.1038/sj.onc.1208559

Saitou, M., Barton, S.C., Surani, M.A., 2002. A molecular programme for the specification of germ cell fate in mice. Nature 418, 293–300. https://doi.org/10.1038/nature00927
Saitou, M., Payer, B., O'Carroll, D., Ohinata, Y., Surani, M.A., 2005. Blimp1 and the Emergence of the Germ Line during Development in the Mouse. Cell Cycle 4, 1736–1740. https://doi.org/10.4161/cc.4.12.2209
Saitou, M., Yamaji, M., 2012. Primordial Germ Cells in Mice. Cold Spring Harb Perspect Biol 4, a008375. https://doi.org/10.1101/cshperspect.a008375
Sasaki, H., Matsui, Y., 2008. Epigenetic events in mammalian germ-cell development: reprogramming and beyond. Nat Rev Genet 9, 129–140. https://doi.org/10.1038/nrg2295
Schrans-Stassen, B.H.G.J., van de Kant, H.J.G., de Rooij, D.G., van Pelt, A.M.M., 1999. Differential Expression of c-kit in Mouse Undifferentiated and Differentiating Type A Spermatogonia. Endocrinology 140, 5894–5900. https://doi.org/10.1210/endo.140.12.7172
Seita, J., Weissman, I.L., 2010. Hematopoietic stem cell: self-renewal versus differentiation. WIREs Systems Biology and Medicine 2, 640–653. https://doi.org/10.1002/wsbm.86
Shami, A.N., Zheng, X., Munyoki, S.K., Ma, Q., Manske, G.L., Green, C.D., Sukhwani, M., Orwig, K.E., Li, J.Z., Hammoud, S.S., 2020. Single-Cell RNA Sequencing of Human, Macaque, and Mouse Testes Uncovers Conserved and Divergent Features of Mammalian Spermatogenesis. Developmental Cell 54, 529-547.e12. https://doi.org/10.1016/j.devcel.2020.05.010
Sharma, M., Braun, R.E., 2018. Cyclical expression of GDNF is required for spermatogonial stem cell homeostasis. Development 145, dev151555. https://doi.org/10.1242/dev.151555
Shinohara, T., Avarbock, M.R., Brinster, R.L., 1999. β1- and α6-integrin are surface markers on mouse spermatogonial stem cells. Proceedings of the National Academy of Sciences 96, 5504–5509. https://doi.org/10.1073/pnas.96.10.5504
Shinohara, T., Orwig, K.E., Avarbock, M.R., Brinster, R.L., 2001. Remodeling of the postnatal mouse testis is accompanied by dramatic changes in stem cell number and niche accessibility. Proceedings of the National Academy of Sciences 98, 6186–6191. https://doi.org/10.1073/pnas.111158198
Shinohara, T., Orwig, K.E., Avarbock, M.R., Brinster, R.L., 2000. Spermatogonial stem cell enrichment by multiparameter selection of mouse testis cells. Proceedings of the National Academy of Sciences 97, 8346–8351. https://doi.org/10.1073/pnas.97.15.8346
Shirakawa, T., Yaman-Deveci, R., Tomizawa, S., Kamizato, Y., Nakajima, K., Sone, H., Sato, Y., Sharif, J., Yamashita, A., Takada-Horisawa, Y., Yoshida, S., Ura, K., Muto, M., Koseki, H., Suda, T., Ohbo, K., 2013. An epigenetic switch is crucial for spermatogonia to exit the undifferentiated state toward a Kit-positive identity. Development 140, 3565–3576. https://doi.org/10.1242/dev.094045
Smith, B.E., Braun, R.E., 2012. Germ Cell Migration Across Sertoli Cell Tight Junctions. Science 338, 798–802. https://doi.org/10.1126/science.1219969
Sohni, A., Tan, K., Song, H.-W., Burow, D., de Rooij, D.G., Laurent, L., Hsieh, T.-C., Rabah, R., Hammoud, S.S., Vicini, E., Wilkinson, M.F., 2019. The Neonatal and

Adult Human Testis Defined at the Single-Cell Level. Cell Reports 26, 1501-1517.e4. https://doi.org/10.1016/j.celrep.2019.01.045
Speed, R.M., 1982. Meiosis in the foetal mouse ovary. Chromosoma 85, 427–437. https://doi.org/10.1007/BF00330366
Strohmeyer, T., Reese, D., Press, M., Ackermann, R., Hartmann, M., Slamon, D., 1995. Expression of the c-kit Proto-Oncogene and Its Ligand Stem Cell Factor (SCF) in Normal and Malignant Human Testicular Tissue. The Journal of Urology 153, 511–515. https://doi.org/10.1097/00005392-199502000-00073
Suzuki, H., Sada, A., Yoshida, S., Saga, Y., 2009. The heterogeneity of spermatogonia is revealed by their topology and expression of marker proteins including the germ cell-specific proteins Nanos2 and Nanos3. Developmental Biology 336, 222–231. https://doi.org/10.1016/j.ydbio.2009.10.002
Suzuki, S., McCarrey, J.R., Hermann, B.P., 2021. An mTORC1-dependent switch orchestrates the transition between mouse spermatogonial stem cells and clones of progenitor spermatogonia. Cell Reports 34, 108752. https://doi.org/10.1016/j.celrep.2021.108752
Takashima, S., Kanatsu-Shinohara, M., Tanaka, T., Morimoto, H., Inoue, K., Ogonuki, N., Jijiwa, M., Takahashi, M., Ogura, A., Shinohara, T., 2015. Functional Differences between GDNF-Dependent and FGF2-Dependent Mouse Spermatogonial Stem Cell Self-Renewal. Stem Cell Reports 4, 489–502. https://doi.org/10.1016/j.stemcr.2015.01.010
Tan, K., Song, H.-W., Wilkinson, M.F., 2020. Single-cell RNAseq analysis of testicular germ and somatic cell development during the perinatal period. Development 147, dev183251. https://doi.org/10.1242/dev.183251
Tan, K., Wilkinson, M.F., 2020. A single-cell view of spermatogonial stem cells. Current Opinion in Cell Biology, Differentiation and disease 67, 71–78. https://doi.org/10.1016/j.ceb.2020.07.005
Tanaka, H., Pereira, L. a. V.D., Nozaki, M., Tsuchida, J., Sawada, K., Mori, H., Nishimune, Y., 1998. A germ cell-specific nuclear antigen recognized by a monoclonal antibody raised against mouse testicular germ cells. International Journal of Andrology 20, 361–366. https://doi.org/10.1046/j.1365-2605.1998.00080.x
Tokuda, M., Kadokawa, Y., Kurahashi, H., Marunouchi, T., 2007. CDH1 Is a Specific Marker for Undifferentiated Spermatogonia in Mouse Testes1. Biology of Reproduction 76, 130–141. https://doi.org/10.1095/biolreprod.106.053181
Valli, H., Sukhwani, M., Dovey, S.L., Peters, K.A., Donohue, J., Castro, C.A., Chu, T., Marshall, G.R., Orwig, K.E., 2014. Fluorescence- and magnetic-activated cell sorting strategies to isolate and enrich human spermatogonial stem cells. Fertility and Sterility 102, 566-580.e7. https://doi.org/10.1016/j.fertnstert.2014.04.036
Velte, E.K., Niedenberger, B.A., Serra, N.D., Singh, A., Roa-DeLaCruz, L., Hermann, B.P., Geyer, C.B., 2019. Differential RA responsiveness directs formation of functionally distinct spermatogonial populations at the initiation of spermatogenesis in the mouse. Development 146, dev173088. https://doi.org/10.1242/dev.173088
Vergouwen, R.P.F.A., Jacobs, S.G.P.M., Huiskamp, R., Davids, J. a. G., Rooij, D.G. de, 1991. Proliferative activity of gonocytes, Sertoli cells and interstitial cells during

testicular development in mice. Reproduction 93, 233–243. https://doi.org/10.1530/jrf.0.0930233
Wagers, A.J., Weissman, I.L., 2004. Plasticity of Adult Stem Cells. Cell 116, 639–648. https://doi.org/10.1016/S0092-8674(04)00208-9
Walker, W.H., 2003. Molecular Mechanisms Controlling Sertoli Cell Proliferation and Differentiation. Endocrinology 144, 3719–3721. https://doi.org/10.1210/en.2003-0765
Wehrle-Haller, B., 2003. The Role of Kit-Ligand in Melanocyte Development and Epidermal Homeostasis. Pigment Cell Research 16, 287–296. https://doi.org/10.1034/j.1600-0749.2003.00055.x
Western, P.S., Miles, D.C., van den Bergen, J.A., Burton, M., Sinclair, A.H., 2008. Dynamic Regulation of Mitotic Arrest in Fetal Male Germ Cells. Stem Cells 26, 339–347. https://doi.org/10.1634/stemcells.2007-0622
Wetzel, A., Chavakis, T., Preissner, K.T., Sticherling, M., Haustein, U.-F., Anderegg, U., Saalbach, A., 2004. Human Thy-1 (CD90) on Activated Endothelial Cells Is a Counterreceptor for the Leukocyte Integrin Mac-1 (CD11b/CD18)1. The Journal of Immunology 172, 3850–3859. https://doi.org/10.4049/jimmunol.172.6.3850
Willems, A., Batlouni, S.R., Esnal, A., Swinnen, J.V., Saunders, P.T.K., Sharpe, R.M., França, L.R., Gendt, K.D., Verhoeven, G., 2010. Selective Ablation of the Androgen Receptor in Mouse Sertoli Cells Affects Sertoli Cell Maturation, Barrier Formation and Cytoskeletal Development. PLOS ONE 5, e14168. https://doi.org/10.1371/journal.pone.0014168
Wobus, A.M., Boheler, K.R., 2005. Embryonic Stem Cells: Prospects for Developmental Biology and Cell Therapy. Physiological Reviews 85, 635–678. https://doi.org/10.1152/physrev.00054.2003
Wyns, C., Van Langendonckt, A., Wese, F.-X., Donnez, J., Curaba, M., 2008. Long-term spermatogonial survival in cryopreserved and xenografted immature human testicular tissue. Human Reproduction 23, 2402–2414. https://doi.org/10.1093/humrep/den272
Yarden, Y., Kuang, W.J., Yang-Feng, T., Coussens, L., Munemitsu, S., Dull, T.J., Chen, E., Schlessinger, J., Francke, U., Ullrich, A., 1987. Human proto-oncogene c-kit: a new cell surface receptor tyrosine kinase for an unidentified ligand. The EMBO Journal 6, 3341–3351. https://doi.org/10.1002/j.1460-2075.1987.tb02655.x
Yeh, J.R., Zhang, X., Nagano, M.C., 2012. Indirect Effects of Wnt3a/β-Catenin Signalling Support Mouse Spermatogonial Stem Cells In Vitro. PLOS ONE 7, e40002. https://doi.org/10.1371/journal.pone.0040002
Yeh, J.R., Zhang, X., Nagano, M.C., 2011. Wnt5a is a cell-extrinsic factor that supports self-renewal of mouse spermatogonial stem cells. Journal of Cell Science 124, 2357–2366. https://doi.org/10.1242/jcs.080903
Yeh, J.R., Zhang, X., Nagano, M.C., 2007. Establishment of a Short-Term In Vitro Assay for Mouse Spermatogonial Stem Cells1. Biology of Reproduction 77, 897–904. https://doi.org/10.1095/biolreprod.107.063057
Ying, Y., Zhao, G.-Q., 2001. Cooperation of Endoderm-Derived BMP2 and Extraembryonic Ectoderm-Derived BMP4 in Primordial Germ Cell Generation in the Mouse. Developmental Biology 232, 484–492. https://doi.org/10.1006/dbio.2001.0173

Yoshida, S., Sukeno, M., Nakagawa, T., Ohbo, K., Nagamatsu, G., Suda, T., Nabeshima, Y., 2006. The first round of mouse spermatogenesis is a distinctive program that lacks the self-renewing spermatogonia stage. Development 133, 1495–1505. https://doi.org/10.1242/dev.02316
Yoshida, S., Takakura, A., Ohbo, K., Abe, K., Wakabayashi, J., Yamamoto, M., Suda, T., Nabeshima, Y., 2004. Neurogenin3 delineates the earliest stages of spermatogenesis in the mouse testis. Developmental Biology 269, 447–458. https://doi.org/10.1016/j.ydbio.2004.01.036
Yoshinaga, K., Nishikawa, S., Ogawa, M., Hayashi, S., Kunisada, T., Fujimoto, T., Nishikawa, S., 1991. Role of c-kit in mouse spermatogenesis: identification of spermatogonia as a specific site of c-kit expression and function. Development 113, 689–699. https://doi.org/10.1242/dev.113.2.689
Zhang, X., Ebata, K.T., Nagano, M.C., 2003. Genetic Analysis of the Clonal Origin of Regenerating Mouse Spermatogenesis Following Transplantation1. Biology of Reproduction 69, 1872–1878. https://doi.org/10.1095/biolreprod.103.019273
Zhao, G.-Q., Garbers, D.L., 2002. Male Germ Cell Specification and Differentiation. Developmental Cell 2, 537–547. https://doi.org/10.1016/S1534-5807(02)00173-9
Zheng, Y., Thomas, A., Schmidt, C.M., Dann, C.T., 2014. Quantitative detection of human spermatogonia for optimization of spermatogonial stem cell culture. Human Reproduction 29, 2497–2511. https://doi.org/10.1093/humrep/deu232
Zhou, Z., Shirakawa, T., Ohbo, K., Sada, A., Wu, Q., Hasegawa, K., Saba, R., Saga, Y., 2015. RNA Binding Protein Nanos2 Organizes Post-transcriptional Buffering System to Retain Primitive State of Mouse Spermatogonial Stem Cells. Developmental Cell 34, 96–107. https://doi.org/10.1016/j.devcel.2015.05.014
Zohni, K., Zhang, X., Tan, S.L., Chan, P., Nagano, M., 2012. CD9 Is Expressed on Human Male Germ Cells That Have a Long-Term Repopulation Potential after Transplantation into Mouse Testes1. Biology of Reproduction 87, 27, 1–8. https://doi.org/10.1095/biolreprod.112.098913

5.1 Software used

FlowJo™ Software for Windows Version 10.7.1 & 10.8.1. Becton, Dickinson and Company; 2023.

R Core Team (2022). R: A language and environment for statistical computing. R Foundation for Statistical Computing, Vienna, Austria.

H. Wickham. ggplot2: Elegant Graphics for Data Analysis. Springer-Verlag New York, 2016.

Lenth R (2023). _emmeans: Estimated Marginal Means, aka Least-Squares Means_. R package version 1.8.5, <https://CRAN.R-project.org/package=emmeans>.

Gu Z, Eils R, Schlesner M (2016). “Complex heatmaps reveal patterns and correlations in multidimensional genomic data.” Bioinformatics. doi:10.1093/bioinformatics/btw313.

6. Appendix

6.1 List of primers for RT-qPCR

Gene	Forward	Reverse	Reference
Gfra1	GTGGCAATGACCTGGAAGAT	ATTGCCAAAGGCTTGAATTG	(Grisanti et al., 2009)
Id4	CTACCATCCCGCCCAACAAG	CTCAGCAAAGCAGGGTGAGT	
Etv5	CATCCTACATGAGAGGCGGG	TCCTGCTTGACTTTGCCTTCC	
Nanos2	TCCCATCCTGAGGCACTATGT	ACTGCTGTTGAGTGGACAATAC	(Zhou et al., 2015)
Zbtb16	CGAGCTTCCGGACAACGA	TTGGCACCCGCTGAATG	(Lovelace et al., 2016)
Nanos3	TGTAAGGCTGGATCCCAAAC	CTGATAGATGGCACGGGACT	
Neurog3	GCTATCCACTGCTGCTTGA	CCGGGAAAAGGTTGTTGTGT	(Yoshida et al., 2004)
Sohlh2	GGATTAAAGGCCCCGTTGTC	ATCGCTCTTCCTCCCCTTGA	(Morimoto et al., 2019)
Sohlh1	AGCGGGCCAATGAGGATTAC	CTGCGTTCTCTCTCGCTGAC	(Makino et al., 2019)
Kit	TGGGAGTTTCCCAGAAACAG	AAATGGGCACTTGGTTTGAG	(Yeh et al., 2012)
Stra8	CTCTCCCACTCCTCCTCCA	GAGGTCCATGGTCTGCTTGTA	(Hermann et al., 2015)
Wt1	GAGAGCCAGCCTACCATCC	GGGTCCTCGTGTTTGAAGGAA	
Actb	CCCTAAGGCCAACCGTGAAA	AGCCTGGATGGCTACGTACA	(Hermann et al., 2015)

6.2 Extended Protocol for FC, FACS, and Intracellular FC

1. Weigh Collagenase I and IV (5 mg each) in a 10 mL snap cap tube. Then, weigh DNase I (10 mg) in another tube.

Name	**Final concentration**	**Total amount**
Collagenase I	1 mg/ml	5 mg in 5 mL HBSS
Collagenase IV	1 mg/ml	5 mg in 5 mL HBSS
DNase I	5 mg/ml	10 mg in 2 mL HBSS

2. Prepare 2 x 60mm petri dishes. Add 7 ml PBS in each dish and leave next to dissecting microscope.

3. Euthanize mouse pups by decapitation with scissors up to P9, and isoflurane/CO2 for older pups. Acquire testes and transfer to petri dish.

4. Separate testes from surrounding tissue with scissors. Do not remove tunica yet. Dry testis with kimwipe and weigh. Record weight. Transfer testes to second petri dish.

5. Remove tunica with forceps from all testes. Transfer tunica to first petri dish. Pull apart the seminiferous tubules, gently. Try to minimize damage to tubules.

6. Place all tubules on the wall of a new 15 mL Falcon tube. Bring tube to a biosafety cabinet.

7. Add 5 mL HBSS to snap cap tube containing collagenase. HBSS solution should have been pre-warmed, or alternatively, collagenase solution can be warmed now in a water bath. Mix well by pipetting and transfer solution through 0.2 µm filter into Falcon tube containing testes. Gently shake tube. Testes should be resuspended in the solution, then travel to the bottom of the tube.

8. Incubate tube in 37°C water bath. Total incubation duration is typically 10-12 min. for pup testes. After initial 5 min., shake tube and observe tubules. After another 5 min., shake tube again.

9. Once digestion is satisfactory (tubules are mostly not visible) remove tube from water bath. Add 7 mL PBS to tube. For P8-9 or P16-18 pup testis cells, wait 10 min. so cells can sediment. For P0-2 testis cells, centrifuge cells at 500 x g for 5 min.

10. Remove supernatant (if sedimenting, remove supernatant down to 0.5 mL, being careful not to pick up pellet). Add 7 mL PBS. Repeat sedimentation (or centrifugation for P0-2 testis cells) and remove supernatant.

11. Add 2 mL cell dissociation buffer, up to 3 mL if digesting a particularly large amount of tubules (e.g. 8 or more P16-18 testes). First, incubate at 37°C for 2 min. in water bath (shake tube after first minute). P0-2 cells digest very quickly (may be ready in less than 2 min.) and should typically be ready to move on to DNAse treatment. For other age groups, it typically takes another minute or two in the water bath. Shake tube liberally throughout treatment (around once a minute).

12. Add 1 mL DNase (5 mg/ml) solution to tube, shake briefly, and add 7 mL PBS. For pups, long DNase treatment is unnecessary and dead cell clumps do not form often. Transfer the cell suspension slowly, drop-wise through a 40 µm strainer into a 50 mL Falcon tube. With 2 mL of PBS, wash the original 15 mL tube and transfer solution through strainer.

13. With a 10 mL pipette, transfer the content into a new 15 mL Falcon tube and record the amount of cell solution. Count cells and record. Centrifuge cells at 500 x g for 5 min.

14. Stain cells with Viability Dye. To stain, first transfer cells from 15 mL tube into a 1 mL Eppendorf tube. Resuspend cells to 1 mL PBS total. Incubate in 1 uL Viability Dye antibody per 1 mL cell solution, with up to 10 x 10^6 cells according to the manufacturer protocol (protocol for Biogems Viability Dye 506). Incubate cells for 5 min. on ice. Centrifuge cells at 500 x g for 5 min.

15. Incubate cells with primary antibodies. Each tube should have 100 uL total volume of PBS + 1% BSA. Up to 2 x 10^6 cells per tube. For instance, you will need three tubes for 5 x 10^6 cells

16. Make antibody mastermix solution. In the original experiment, a panel of THY1, ITGA6, GFRA1, KIT, MHC-I, CD45, and CD74 was used for FACS. Prepare additional controls (like FMO controls) as necessary.

    Refer to section 2.5 for information about antibody concentrations. For Intracellular FC, double the concentration of all antibodies, to counteract the effect that permeabilization has on surface antibodies.

17. Incubate cells for 30 min. on ice with agitation. Lay tubes horizontally on the ice. If setting up a new compensation setting, prepare compensation beads.

18. After 30 min. (25-35 min. ideal), remove tubes from ice and add 1 mL PBS to each tube without pipetting. Centrifuge cells at 500 x g for 5 min.

19. Remove supernatant. If performing intracellular FC, skip to step 21. Resuspend cells in PBS + 1% BSA. Aim for 200-300 uL of solution per 10^6 cells. Transfer cell suspension to round-bottom tubes. Up to ~1.2 mL solution per tube. Prepare labelled collection tubes and put 1 mL of collection medium in each tube (collection medium = PBS + 1% BSA).

20. Bring your tubes to the flow cytometer. Unless you are doing intracellular FC, you can stop here.

21. If you are performing intracellular FC, resuspend the cells in ice-cold 4% paraformaldehyde (PBS) solution. pH of paraformaldehyde solution should be close to 7. Incubate 15 min. on ice with agitation.

22. Centrifuge cells at 500 x g for 5 min. Remove supernatant, add 1 mL PBS, and centrifuge again. Unless stated otherwise, all centrifugations are at 500 x g for 5 min. at 4°C.

23. Resuspend cells in ice-cold 0.1% Triton X-100. Incubate for 5 min. on ice. Centrifuge and remove supernatant. Wash with 1 mL PBS. Centrifuge and remove supernatant.

24. Resuspend in blocking buffer. I used PBS + 1% BSA. Blocking may not be necessary. Centrifuge and remove supernatant.

25. Resuspend in PBS + 1% BSA with primary antibodies (100 uL total volume / tube). Prepare controls as necessary. Incubate 20 min. on ice with agitation (longer duration may work).

26. Add 1 mL PBS in each tube to wash. Centrifuge and remove supernatant. Resuspend in PBS + 1% BSA with secondary antibodies (100 uL total volume / tube). Incubate 10 min. on ice with agitation (longer duration may work).

27. Centrifuge and remove supernatant. Resuspend in PBS + 1% BSA and transfer to round-bottom tubes. Read cells on flow cytometer.

A common problem with the intracellular FC protocol is distortion of the signal of surface antibodies. Some degree of distortion is inevitable during the fixation and permeabilization process. However, the distortion may be so extreme such that the entire fractions disappear (e.g. Fraction A). If this is the case, you can try different adjustments in the protocol. Some examples are to reduce washing steps, change permeabilization agent, or modify fixation duration.

6.3 Flow cytometric profiles throughout prepubertal development.

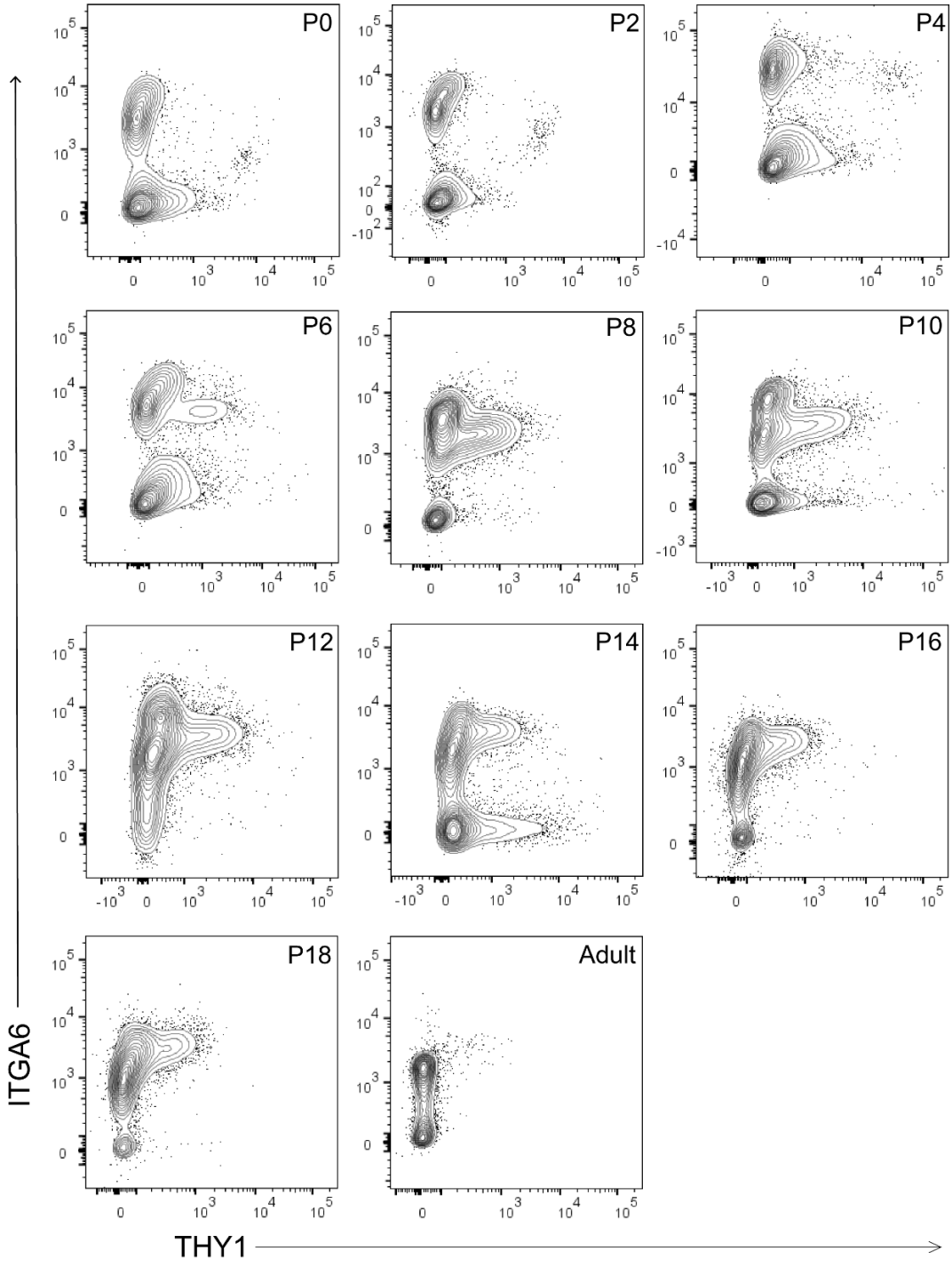

Figure 13. Flow cytometric profiles (THY1/ITGA6) of ROSA26 pups throughout postnatal development change gradually. Profiles of 11 different stages are shown. Expression intensity of markers should not be compared between stages, as not all profiles were acquired on the same machine and setting. Notably, the profiles for P4, P10, P12, and P14 were acquired on the BD LSRFortessa while all other profiles were acquired on the FACSAria Fusion.

6.4 KIT expression increases in both Fraction A and Fraction C during postnatal development.

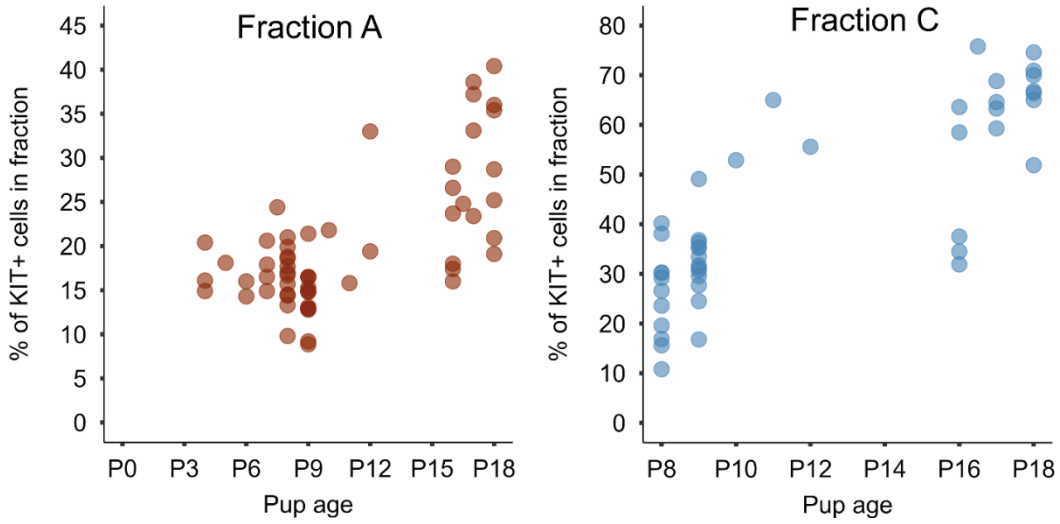

Figure 14. Percentage (%) of KIT-expressing cells in Fraction A and C throughout postnatal development. Data for Fraction C starts at P8 because it is nonexistent before that age. KIT-expressing cells increase in both Fraction A and Fraction C postnatally, at least until P18. Averages for Fraction A: 15.3% ± 0.6% at P8-9 and 27.4% ± 1.8% at P16-18. Averages for Fraction C: 29.2% ± 1.8% at P8-9 and 61.4% ± 3.3% at P16-18.

6.5 RT-qPCR data of genes not displayed in Figure 10

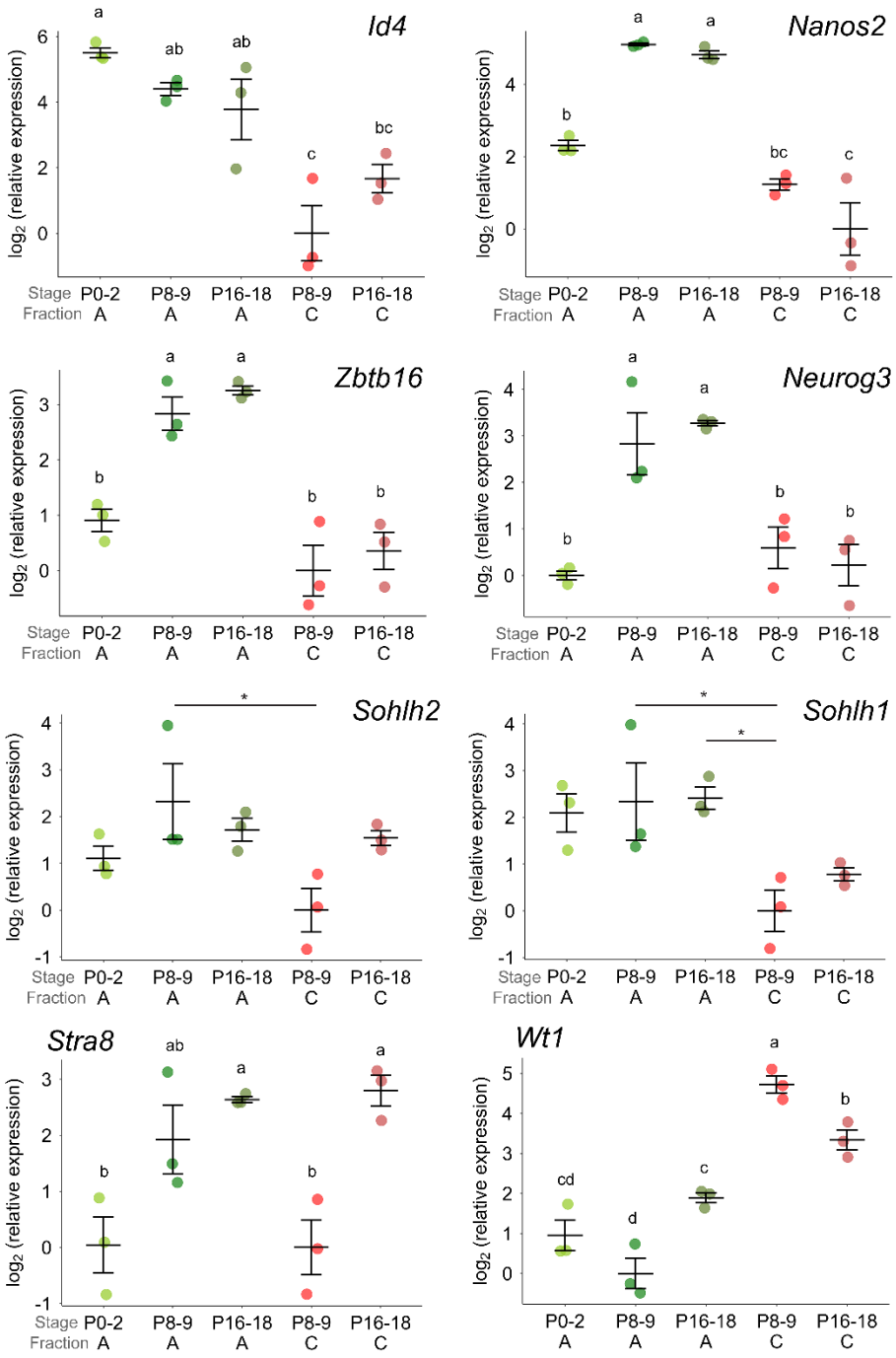

Figure 15. RT-qPCR data of eight genes that were not displayed in Figure 10. Relative expression of genes in Fractions A and C at the three developmental stages, measured with RT-qPCR. Mean expression was compared with a one-way ANOVA and pairwise comparisons were conducted with Tukey's HSD (* $p < 0.05$; ** $p < 0.01$; *** $p < 0.001$). Alphabet labels ('a', 'b', 'c') indicate statistical significance between two labels with distinct letters. For example, there is a significant difference between 'ab' and 'c', but no difference between 'ab' and 'b'.

6.6 Copyright permissions

Figure 1. Organization of the seminiferous epithelium. Adapted from de Rooij, 2017. Reproduced with permission from Springer Nature.

SPRINGER NATURE LICENSE
TERMS AND CONDITIONS

May 01, 2023

This Agreement between Youngmin Song ("You") and Springer Nature ("Springer Nature") consists of your license details and the terms and conditions provided by Springer Nature and Copyright Clearance Center.

License Number	5540040284821
License date	May 01, 2023
Licensed Content Publisher	Springer Nature
Licensed Content Publication	Springer eBook
Licensed Content Title	Organization of the Seminiferous Epithelium and the Cycle, and Morphometric Description of Spermatogonial Subtypes (Rodents and Primates)
Licensed Content Author	Dirk G. de Rooij Ph.D.
Licensed Content Date	Jan 1, 2017
Type of Use	Thesis/Dissertation
Requestor type	academic/university or research institute
Format	print and electronic
Portion	figures/tables/illustrations
Number of figures/tables /illustrations	1

Figure 4. Scheme of two distinct prospermatogonial populations in mouse. Adapted from McCarrey, 2017. Reproduced with permission from Springer Nature.

SPRINGER NATURE LICENSE
TERMS AND CONDITIONS

May 26, 2023

This Agreement between Youngmin Song ("You") and Springer Nature ("Springer Nature") consists of your license details and the terms and conditions provided by Springer Nature and Copyright Clearance Center.

License Number	5556350521863
License date	May 26, 2023
Licensed Content Publisher	Springer Nature
Licensed Content Publication	Springer eBook
Licensed Content Title	Transition of Prenatal Prospermatogonia to Postnatal Spermatogonia
Licensed Content Author	John R. McCarrey Ph.D.
Licensed Content Date	Jan 1, 2017
Type of Use	Thesis/Dissertation
Requestor type	academic/university or research institute
Format	print and electronic
Portion	figures/tables/illustrations
Number of figures/tables /illustrations	1

Figure 5. Expression of genes at various stages of SSC development, as revealed by scRNA-seq. Adapted from Tan et al., 2020. Reproduced with permission (Development, The Company of Biologists).

CCC Marketplace

This is a License Agreement between Youngmin Song ("User") and Copyright Clearance Center, Inc. ("CCC") on behalf of the Rightsholder identified in the order details below. The license consists of the order details, the Marketplace Permissions General Terms and Conditions below, and any Rightsholder Terms and Conditions which are included below.

All payments must be made in full to CCC in accordance with the Marketplace Permissions General Terms and Conditions below.

Order Date	01-May-2023	Type of Use	Republish in a thesis/dissertation
Order License ID	1350293-1		
ISSN	0950-1991	Publisher	COMPANY OF BIOLOGISTS,
		Portion	Chart/graph/table/figure

LICENSED CONTENT

Publication Title	Development	Country	United Kingdom of Great Britain and Northern Ireland
Author/Editor	COMPANY OF BIOLOGISTS.	Rightsholder	The Company of Biologists Ltd.
Date	01/01/1987	Publication Type	Journal
Language	English		

REQUEST DETAILS

Portion Type	Chart/graph/table/figure	Distribution	Worldwide
Number of Charts / Graphs / Tables / Figures Requested	1	Translation	Original language of publication
Format (select all that apply)	Print, Electronic	Copies for the Disabled?	No
Who Will Republish the Content?	Academic institution	Minor Editing Privileges?	Yes
Duration of Use	Life of current edition	Incidental Promotional Use?	No
Lifetime Unit Quantity	Up to 499	Currency	CAD
Rights Requested	Main product		